T Lymphopoiesis from Pluripotent Stem Cells by Defined Transcription Factors at Single Cell Resolution

Rongqun Guo[1,2,3,5,6,10], Fangxiao Hu[1,2,5,6,10], Qitong Weng[1,2,3,5,6,10], Cui Lv[1,2,5,6], Hongling Wu[1,2,5,6], Lijuan Liu[1,2,4,5,6], Zongcheng Li[7], Yang Zeng[7], Zhijie Bai[7], Mengyun Zhang[1,2,4,5,6], Yuting Liu[1,2,5,6], Xiaofei Liu[1,2,4,5,6], Chengxiang Xia[1,2,3,5,6], Tongjie Wang[1,2,5,6], Peiqing Zhou[1,2,3,5,6], Kaitao Wang[1,2,4,5,6], Yong Dong[1,2,5,6], Yuxuan Luo[8], Xiangzhong Zhang[8], Yuxian Guan[1,2,5,6], Yang Geng[1,2,4,5,6], Juan Du[1,2,3,5,6], Yangqiu Li[9], Yu Lan[9], Jiekai Chen[1,2,3,4,5,6], Bing Liu[7]*, Jinyong Wang[1,2,3,4,5,6]*

[1]CAS Key Laboratory of Regenerative Biology, Guangzhou Institutes of Biomedicine and Health, Chinese Academy of Sciences, Guangzhou, China.

[2]Guangzhou Regenerative Medicine and Health-Guangdong Laboratory (GRMH-GDL), Guangzhou, China.

[3]University of Chinese Academy of Sciences, Beijing, China.

[4]Joint School of Life Sciences, Guangzhou Institutes of Biomedicine and Health, Guangzhou Medical University, Guangzhou, China.

[5]Guangdong Provincial Key Laboratory of Stem cell and Regenerative Medicine, Guangzhou Institutes of Biomedicine and Health, Chinese Academy of Sciences, Guangzhou, China.

[6]Institute for Stem Cell and Regeneration, Chinese Academy of Sciences, Beijing, China.

[7]State Key Laboratory of Proteomics, Translational Medicine Center of Stem Cells, Fifth Medical Center, General Hospital of PLA, Beijing, China.

[8]Department of Hematology, the Third Affiliated Hospital of Sun Yat-Sen University, Guangzhou, China.

[9]Key Laboratory for Regenerative Medicine of Ministry of Education, Institute of Hematology, School of Medicine, Jinan University, Guangzhou, China.

[10]These authors contributed equally.

*e-mail: wang_jinyong@gibh.ac.cn; bingliu17@yahoo.com

ABSTRACT

To date, preferentially regenerating T lymphopoiesis *in vivo* from pluripotent stem cells (PSC) remains a practical challenge. Here we documented that synergistic expression of Runx1 and Hoxa9 during endothelial to hematopoietic transition stage preferentially generated hematopoietic progenitors capable of homing to thymus and outputting full T lymphopoiesis in primary and secondary recipients. Single-cell transcriptome and functional analyses illustrated the cellular trajectory of T lineage induction from PSC, unveiling the T-lineage specification determined at as early as hemogenic endothelial cell stage and the *bona fide* pre-thymic progenitors with thymus-homing traits. The mature iT cells distributed normally in central and peripheral lymphoid organs and exhibited abundant TCRαβ repertoire. Furthermore, the TCR-edited PSC produced functional tumor-specific-TCR-T cells in vivo that effectively eradicated tumor cells and transformed to memory cells. This study provides insight into preferential and complete lymphopoiesis from PSC.

Key Words: Pluripotent stem cells, transcription factors, *Runx1*, *Hoxa9*, T lymphopoiesis

INTRODUCATION

Engineered T cells, such as chimeric antigen receptor (CAR)-T cells (*1*) and tumor antigen-specific T cell receptor (TCR)-T cells (*2*), have been broadly applied in anti-tumor therapies (*3, 4*). Currently, patient blood-derived T cells are the major cell source for this type of cell therapy, the availability of which seriously depends on the conditions of individual patients and disease contexts. Regarding the unlimited source and gene-editing advantages of induced pluripotent stem cells (iPSC) (*5*), generating functional T cells from iPSC provides an ideal approach for broadening T cell-based translational applications.

A canonical method to generate T cells *in vitro* is via co-culture of hematopoietic stem/progenitors (HSPC) with stromal cell lines expressing the Notch ligand, such as OP9-DL1/DL4 or 3D-based MS5-hDLL1/4 (*6-8*). It has been previously shown that Notch ligands can mature mouse natural $Sca1^{+}cKit^{+}$ and human natural $CD34^{+}$ blood progenitor cells to $CD7^{+}$ pre-thymic cells that can colonize thymi *in vivo* and mature into functional T cells (*9, 10*). However, this approach generated induced T cell progenitors from PSC lacked homing capacity *in vivo* and could only reconstitute functional T lymphopoiesis *in vivo* when pre-embedded in congenic fetal thymic lobes (*11*). Another prevailing concept for generating functional T lymphopoiesis from PSC is via induction of hematopoietic stem cell-like intermediates by defined factors (*12-15*). However, generating robust *bona fide* induced-HSC (iHSC) from PSC remains inefficient (*16, 17*). Accumulated developmental evidence shows that blood progenitors prior to the occurrence of definitive HSC, also possess T cell lineage differentiation

potential (*18-20*). Despite the abundant knowledge of the pivotal transcription factors regulating T cell development from HSC derivatives (*21*), intrinsic determinants of T cell lineage potential in the HSC-independent hematopoietic progenitors at the pre-liver and pre-thymus stages remain elusive. Thus, identifying such crucial T lineage-potential determinants might help to establish a solid protocol for efficiently reconstituting T lymphopoiesis from PSC.

In this study, we identified that the coordinated expression of exogenous *Runx1* and *Hoxa9* during the endothelial to hematopoietic transition stage resulted in a type of induced hemogenic endothelial cells (iHEC) resembling the developmental E11 AGM endothelial cells and pre-HSC (*22*). The single iHEC can be robustly educated into induced hematopoietic progenitor cells (iHPC), which gave rise to induced T cells (iT cells) with abundant TCRαβ repertoire *in vivo*. The iT cells developed in thymus and distributed into central and peripheral lymphoid organs. The iT cells exhibited adaptive immune response and formed immune memory. Therapeutically, these iT cells possessed anti-tumor activities *in vivo* when engineered to carry tumor antigen-specific TCR at PSC stage. We established a novel approach of preferentially reconstituting functional and therapeutic T lymphopoiesis *in vivo* from PSC by defined transcription factors, which technically creates a link between the precision gene-edited PSC source and T cell-based immunotherapy for translational purpose.

RESULTS

Reconstitution of T Lymphopoiesis *in vivo* from Inducible *Runx1-p2a-Hoxa9*-Embryonic Stem Cells

We hypothesized that the lymphogenic potential is determined by intrinsic determinants at putative endothelial precursor cell stage prior to and independent of HSC formation. Therefore, enforced expression of these master determinants might direct lymphoid differentiation from PSC. Since *Runx1* is pivotal for endothelial to hematopoietic transition (EHT) (*23-25*), definitive hematopoietic development (*26-28*) and T cell development (*21*), we started from evaluating the potential effect of *Runx1* in lymphogenic commitment from PSC. To avoid the expression variations introduced by viral delivery systems, we inserted the inducible expression cassette of *Runx1* into the *Rosa26 locus* of embryonic stem cells (*iRunx1*-ESC, C57BL/6 background) by homologous recombination (Figure S1A), which resulted in the conditional expression of exogenous *Runx1* in the presence of doxycycline (Figure S1B). We used AFT024-(mSCF/mIL3/mIL6/hFlt3L) cell line-cultured supernatants as conditioned medium (CM) for the *in vitro* induction of iHEC and subsequent iHPC, as AFT024 CM is beneficial for the generation of induced HPC *in vitro* (*29*). To functionally assess the T lymphopoiesis potential of iHPC, we transplanted the bulk cells containing abundant iHPC (referred as iHPC thereafter) into irradiated (2.25 Gy) B-NDG recipients (iHPC recipients) and used the occurrence of $CD3^+$ cells in peripheral blood (PB) as a positive readout of induced T lymphopoiesis *in vivo* (Figure 1A). Based on a modified protocol for HEC induction from PSC (*30*), we successfully generated iHEC and hematopoietic

progenitor derivatives (Figures S1C-S1E). However, the *iRunx1*-ESC derivatives eventually failed to generate T cells on the conditions of either *in vitro* OP9-DL1 co-culture system (Figure S1F) or *in vivo* transplantation setting (Figure S1G). We speculated that the other transcription factors essential for T lineage generation might be absent in the *iRunx1*-ESC derivatives. To identify these absent factors, we sorted the single iHEC from *iRunx1*-ESC and performed single-cell RNA-Seq. In comparison with E11 T1-pre-HSC, we identified eight hematopoietic-essential transcription factors, *Hoxa5* (*13*), *Hoxa7* (*31*), *Hoxa9* (*32*), *Hoxa10* (*33*), *Hlf* (*34*), *Ikzf1* (*35*), *Nkx2-3* (*36*), and *Setbp1* (*37*), which were barely expressed in *iRunx1*-ES-derived iHEC but abundantly expressed in E11 T1-pre-HSC (Figure 1B). Consistent with the previous reports that human PSC-derived HEC lacks expression of HOXA family (*13, 38*). We further used an "*iRunx1+Xi*" tandem-factor-knock-in strategy to perform unbiased screening of the potential combinatory effects of these factors with Runx1 in lymphoid lineage induction. Following the same induction protocol, we identified that the inducible expression of exogenous *Runx1* and *Hoxa9* from day 6 to day 11 during the induction program led to the production of robust iHEC phenotypically resembling embryonic pre-HSC ($CD31^{+}CD41^{low}CD45^{-}c\text{-}kit^{+}CD201^{high}$) (Figure 1C) (*22*). Notably, $CD201^{+/high}$ expression can enrich hemogenic precursors with both definitive HPC and HSC potential from as early as E9.5 embryos (*39*). After co-culture of these iHEC with OP9-DL1 feeder line (GFP^{+}) in the presence of CM and doxycycline (1 μg/ml), robust iHPC occurred at day 21, including phenotypic pre-thymic progenitors ($Lin^{-}c\text{-}kit^{+}CD127^{+}/CD135^{+}$) (*21*) (Figure 1D), and $CD11b^{+}/Gr1^{+}$ myeloid cells, but no $CD3^{+}$

T cells (Figure S1H). To further assess the engraftment potential of these iHPC, we transplanted 0.5-1 million *iR9*-ESC-derived iHPC (day-21) into irradiated (2.25 Gy) B-NDG mice (8-week-old, CD45.1 strain) in the absence of doxycycline. Four weeks after transplantation, we observed donor-derived $CD45.2^+$ $CD3^+$ T cells, but no $CD45.2^+CD19^+$ B cells and no $CD45.2^+CD11b^+$ myeloid cells, in the PB of B-NDG mice transplanted with the iHPC (Figure 1E). Five independent experiments indicated that the *iR9*-ESC-derived iHPC gave rise to $CD3^+$ iT cells in over 80% B-NDG recipients (iT-B-NDG mice, 32/40) (Figures 1F and S1I). In addition, the day-17 iHPC also reconstituted T lymphopoiesis in B-NDG recipients (Figures S2A-2D). Thus, we established a novel approach of preferentially generating iT cells from gene-edited PSC by defined transcription factor *Runx1* and *Hoxa9*.

The iT Cells Show Features of Multi-organ Distributions and Abundant TCR Diversity

We further analyzed the tissue distributions and immunophenotypes of the regenerated T lymphocytes in iT-B-NDG mice. Mature CD4SP and CD8SP iT cells were detected in the spleen, lymph node and PB of iT-B-NDG mice, the majority of which were TCRβ positive (Figure 2A). In addition, γδ iT cells were also detected in gut and lung tissues of iT-B-NDG mice (Figure S3A). Induced NK cells (iNK, $CD45.2^+NK1.1^+CD3^-$) were also detected in the spleen and bone marrow of iT-B-NDG mice (Figure S3B). The thymus of iT-B-NDG mice also contained induced CD4SP (iCD4SP), induced double positive (iDP, $CD45.2^+CD4^+CD8^+$), induced CD8SP (iCD8SP), and induced double negative (iDN, $CD45.2^+Lin^-CD4^-CD8^-$) cells when examined at week-4 and week-5

after transplantation of iHPC. Interestingly, the majority of the iDN cells were at iDN1 ($CD45.2^+Lin^-CD4^-CD8^-CD44^+CD25^-$) phase at week-4, and at iDN2 ($CD45.2^+Lin^-CD4^-CD8^-CD44^+CD25^+$)/iDN3 ($CD45.2^+Lin^-CD4^-CD8^-CD44^-CD25^+$) phases at week-5 (Figure 2B). Besides the iT cells and induced $NK1.1^+CD3^-$ NK (iNK) cells detected in bone marrow, we also observed *iR9*-ES-derived $Lin^-Sca1^+cKit^+$ (iLSK) progenitor cells (Figure 2C). To assess whether the iLSK cells can contribute to T lymphopoiesis, we sorted this population from primary iHPC recipients (week-6) and performed secondary transplantation. Six weeks after transplantation, iT cells appeared in PB, BM, and SP of the B-NDG recipients (Figure 2D). Of note, despite *iR9*-ES-derived myeloid lineage cells were barely detected *in vivo*, the iLSK cells indeed gave rise to very limited myeloid colonies in CFU assay (data not shown). To further characterize the iT cells at transcriptome level, we sorted 1,000 cell aliquots of the CD4SP iT cells and CD8SP iT cells from the spleens of iT-B-NDG mice for RNA-Seq analysis. Our data indicated that the CD4SP iT cells resembled natural CD4SP T cells, and the CD8SP iT cells resembled natural CD8SP T cells, both of which expressed surface marker-encoding genes *Cd2*, *Fas*, *Cd3e*, *Cxcr3*, *Cd28*, *Cd27*, *Cd7*, *Cd5*, and *Il7r* (Figure 2E). Of note, the CD4SP iT cells, but not CD8SP iT cells, expressed the *ThPOK* (T helper inducing POK factor, also known as *Zbtb7b*), a master regulator in regulating CD4 vs. CD8 T cell lineage commitment (*40*). In addition, the iT cells also expressed T cell identity genes and key regulators *Tcf7* (*41*), *Tox* (*42*), *Lck* (*43*), *Gata3* (*44*), *Bcl11b* (*45*), *Ikzf2* (*46*), and *Rora* (*47*) (Figure 2F). In comparison with natural T cell counterparts, the iT cells also showed features of discrepantly expressed genes (a difference in expression

of over two-fold; adjusted P value < 0.05 (DESeq2 R package)) (Supplementary file 1), including weaker expression of *Tcf7*. Genomic PCR sequencing using primer pairs flanking the *Runx1-p2a-Hoxa9* element further confirmed that the reconstituted iT cells *in vivo* were of *iR9*-PSC origin, which carried the inserted *Runx1-p2a-Hoxa9* (Figure S3C). To further assess the diversities of the TCRαβ clonotypes of the iT cells, we performed TCR deep sequencing using the sorted naïve CD4SP ($CD45.2^+CD4^+CD62L^+CD44^-$) and CD8SP iT cells ($CD45.2^+CD8^+CD62L^+CD44^-$) from the spleens and thymi of iT-B-NDG mice at week-6 after transplantation of iHPC. The aliquots of 15,000 sorted naïve CD4SP and CD8SP iT cells were used as cell inputs for TCRαβ sequencing at the transcription level. TCRαβ clonotype profiling using MiXCR (*48*) captured abundant diversities of TCRαβ sequences among the sorted naïve iT cells isolated from the thymi (Figures 2G and 2H) and spleens (Figures 2I and 2J) of the iT-B-NDG mice. Collectively, these data indicate that the *iR9*-ESC-derived iHPC reconstitute T lymphopoiesis *in vivo* resembling natural T cell development.

Single iHEC Efficiently Give Rise to iT Cells both *in vitro* and *in vivo*

To further investigate the efficiency of iHEC differentiating into iT cells, we sorted single iHEC into individual wells (24 well-plates) pre-seeded with OP9-DL1 feeder cells (Figure 3A). After ten-day co-culture, over 15 percent individual iHEC formed blood colonies (76/384 wells) (Figure 3B), which contained abundant pre-thymic progenitors ($Lin^-c\text{-}kit^+CD127^+/CD135^+$) (Figure S4). After co-culture with OP9-DL1 feeder line in the presence of hFlt3L, hIL7 and doxycycline (1 μg/ml), these iHEC-formed blood colonies (30/30) further differentiated into $CD3^+$ iT cells *in vitro* (Figure

197 3B), including a major population of TCRγδ iT cells, and a small proportion of $CD8^+$
198 TCRβ iT cells (Figure 3C). To assess the T lymphopoiesis potential of these single-
199 iHEC-derived iHPC, we further collected the iHPC from each colony at day 21 and
200 transplanted them into individual B-NDG mice. Four weeks after transplantation,
201 $CD11b^-CD19^-CD3^+$ iT cells were detected in approximately 28% (7/25) B-NDG mice
202 transplanted with the cell derivatives from individual iHEC-formed clones (Figures 3B
203 and 3D**)**. Collectively, the *iR9*-ESC-derived iHEC robustly gave rise to T cells at the
204 single cell level.

205 **Cellular trajectory from iHEC and iHPC**

206 To characterize the single iHEC at transcriptome level, we performed single-cell RNA-
207 Seq using the sorted iHEC and compared them with natural single E11 endothelial cells
208 (EC), Type-I pre-HSC, Type-II pre-HSC, E12 HSC, E14 HSC, and adult HSC described
209 previously (*22*). Principle component analysis indicated that the iHEC localized
210 between embryonic EC and pre-HSC **(**Figures 4A and 4B**)**. A large proportion of iHEC
211 expressed artery or vein-related genes, suggestive of their EC-like nature (Figure 4C).
212 Most iHEC expressed endothelial surface marker-encoding genes *Cdh5* (coding VE-
213 Cadherin, 70/70) and *Esam* (57/70), which were continuously expressed from
214 embryonic EC to pre-HSC at a relatively high level. On the other hand, partial iHEC
215 expressed *Procr* (coding CD201, 32/70), *Cd47* (33/70) and *Cd63* (44/70), which were
216 upregulated from EC to pre-HSC (Figure 4D). The expression of transcription factors
217 related to endothelial and hematopoietic development further revealed that the iHEC
218 shared a similar feature with embryonic EC and pre-HSC. Majority of the iHEC

219 expressed *Fli1* (66/70), *Erg* (42/70), *Lmo2* (49/70), *Mycn* (65/70), and *Sox7* (38/70).
220 Specifically, a small proportion of iHEC expressed *Bcl11a* (11/70) and *Hoxb5* (24/70).
221 All these transcription factors are pivotal for lymphoid lineage development (Figure
222 4E). Thus, the molecular features of the iHEC show similarities with embryonic EC
223 and pre-HSC.

224 To further characterize the iHPC during the hematopoietic maturation process, we
225 sorted the single iHPC from day-14, day-17, day-21 cell products derived from *iR9*-ES
226 and performed single-cell RNA-Seq. To visualize the time course data of iHPC, we
227 performed t-distributed stochastic neighbor embedding (tSNE, the genes with
228 expression value TPM >1 in more than 30 samples were selected) analysis and
229 illustrated that the day-14-iHPC formed a unique population distinct from day-11-iHEC
230 and the major population of day-17 iHPC. However, the day-17 iHPC and day-21 iHPC
231 already merged (Figure 4F). In addition, the day-21 iHPC formed a new subpopulation
232 labeled with relatively abundant *Gata2* expression (Figure S5A). The endothelia-
233 related transcription factors, such as Sox7 and Sox18, were abundantly expressed in
234 day-11 iHEC, however, were immediately silenced in day-14 iHPC (Figure 4G). The
235 *Ets1* gene, involving embryonic endothelial and lymphoid development (*49*), was shut
236 down in day-14 iHPC but turned on again in day-17 iHPC (Figure 4G). The
237 transcription factors involving hematopoietic development, such as *Lyl1* (*50*), *Etv6* (*51*),
238 *Prdm5* (*14*), *Myb* (*52*), *Sfpi1* (*53-55*), and *Meis1* (*56*), were widely expressed among
239 day-14, 17, and 21 iHPC populations. (Figure 4H). Further, the transcription factors
240 related to lymphoid development, including *Lmo2* (*57*), *Bcl11a* (*58*), *Ikzf1* (*59*), *Myc*

(*21, 60*), *Gata3* (*61*), and *Tcf7* (*41*), were also expressed in iHPC (Figures 4I and S5B). Of note, day-17 and day-21 iHPC showed abundant expression of *Tcf7* (Figure 4I). Given the thymus-homing problem of the PSC-derived HPC reported by others (*11*), we observed that the day-21-iHPC derived from *iR9*-ES abundantly expressed surface marker-encoding gene *Kit* (*21*), *Flt3* (*21*), *Cd7* (*9, 10*), *Ccr9* (*62, 63*), and *Cxcr4* (*64, 65*), which is a feature of natural pre-thymic progenitors possessing thymus-homing ability (Figure 4I). Collectively, the *iR9*-ES-derived iHPC show hematopoietic or lymphopoietic features at transcriptome level and the day-21 iHPC contain robust pre-thymic progenitor-like cells.

The iT Cells Reject Allogeneic Skin and Form Memory Response *in vivo*

To investigate the function of iT cells derived from *iR9*-ESC (C57BL/6 background) *in vivo*, we transferred the iT cells (5 million equivalents of iT cells per *Rag1*$^{-/-}$) isolated from iT-B-NDG spleen into *Rag1*$^{-/-}$ mice (iT-*Rag1*$^{-/-}$ mice). Four days after the adoptive iT cell transfer, we transplanted allogeneic skin from BALB/c mice into the iT-*Rag1*$^{-/-}$ mice. The allogeneic skin grafts were rapidly rejected by iT-*Rag1*$^{-/-}$ mice at around day 9 after transplantation, as indicated by bulged, ulcerative and necrotic lesions at the graft sites (Figure 5A). Besides the mature iT cells (CD4SP, CD8SP) in the PB of iT-*Rag1*$^{-/-}$ mice (Figure 5B), activated CD4SP and CD8SP iT cells (CD44^{high}CD69^{+}) were also detected in the rejected allogeneic skin tissues (Figure 5C). The iT-*Rag1*$^{-/-}$ mice still showed the existence of iT cells in PB thirty days after the primary allogeneic rejection, and again rejected the secondary allogenic skin grafts (Figure S6). Flow cytometry indicated that IL17^{+} and IFNγ^{+} CD4^{+} iT cells, and IFNγ^{+}

263 $CD8^+$ iT cells existed in the primary- and secondary-rejected skin grafts (Figure 5D).
264 Collectively, these results indicated that the adoptively transferred iT cells in *Rag1*$^{-/-}$
265 mice mediated rejection of allogeneic skin grafts and sustained immunological
266 memory, suggestive of a typical adaptive immune response.

267 **The iT Cells Derived from TCR-edited iPSC eradicate tumor cells *in vivo***

268 Regarding the advantages of unlimited cell source and gene-editing advantage of iPSC,
269 we introduced tumor antigen-specific TCR (MHC-I restricted OVA TCR, OT1) into
270 *iR9*-iPSC and further assessed the anti-tumor activity of the derived OT1 iT cells. We
271 reprogrammed mouse MEF (C57BL/6 background, CD45.2 strain) into iPSC using
272 retro-viruses carrying *Oct4*/*Klf4*/*Sox2*. Two cassettes of *rtTA-TRE-Runx1-p2a-Hoxa9-*
273 *HygroR* and *CAG-OT1-TCR-IRES-GFP-PuroR* were inserted into the loci of *Rosa26*
274 and *Hipp11* of iPSC (*OT1-iR9*-iPSC), respectively (Figure 6A). Intracellular staining
275 indicated that the OT1-TCR were expressed in the *OT1-iR9*-iPSC (Figure 6B). The
276 *OT1-iR9*-iPSC were further induced into OT1-iHEC (Figure 6C) and OT1-iHPC
277 (Figure 6D). We transplanted the OT1-iHPC (three million per mouse) into irradiated
278 (4.5 Gy) *Rag1*$^{-/-}$ mice (OT1-iHPC recipients) to reconstitute OT1-iT lymphopoiesis.
279 Six weeks after transplantation, the OT1-iHPC recipients showed GFP^+CD8^+ iT cells
280 expressing OT1 TCRαβ in PB (Figure 6E). We then engrafted E.G7-OVA tumor cells
281 into the groin of the *Rag1*$^{-/-}$ or OT1-iT reconstituted *Rag1*$^{-/-}$ mice (OT1-iT-*Rag1*$^{-/-}$ mice)
282 by subcutaneous injection (0.2 million/mouse). Tumor growth kinetics demonstrated
283 that the E.G7-OVA tumors were dramatically inhibited in the OT1-iT-*Rag1*$^{-/-}$ mice in
284 comparison with the control *Rag1*$^{-/-}$ mice (Figure 6F). We sacrificed the OT1-iT-*Rag1*$^{-}$

285 $^{-/-}$ mice for the distribution analysis of the iT cells in tumors and lymphoid organs 19
286 days after the tumor cell transplantation. Flow cytometry analysis demonstrated that the
287 E.G7-OVA tumors in the OT1-iT-*Rag1*$^{-/-}$ mice were infiltrated with CD8^{+} OT1-iT cells,
288 which contained effector (CD44^{+} CD62L^{-}) and memory (CD44^{+} CD62L^{+}) iT cells, and
289 IFNγ-secreting iT cells (Figure 6G). We also observed abundant CD8^{+} iT cells carrying
290 OT1 TCRαβ in the bone marrow, lymph node, and spleen of these mice (Figure S7).
291 Collectively, these data indicate that the iT cells derived from TCR-engineered iPSC
292 show anti-tumor activity in a solid tumor model.

293 **DISCUSSION**

294 In this study, the iHEC from *iR9*-PSC gave rise to blood progenitor cells preferentially
295 differentiating into iT cells *in vivo*. It is possible that the combinatory expression of
296 *Runx1* and *Hoxa9*, pivotal transcription factors for definitive hematopoietic (*26-28, 66*)
297 and T cell development (*21*), synergistically and preferentially orchestrates the T and
298 NK lineage potentials but intrinsically compromises the other blood lineage potentials
299 during the early EHT and subsequent hematopoietic maturation phases in our induction
300 protocol. Regarding the developmental evidence that an earlier wave of hematopoietic
301 preceding HSC emergence also produces blood progenitors possessing the T cell
302 lineage potential (*18-20*), it is also possible that the *iR9*-PSC-derived iHPC resemble
303 the developmental HPC prior to the occurrence of definitive HSC since overexpression
304 of *Runx1* and *Hoxa9* at definitive HSC phase promoted myeloid-instead of lymphoid-
305 biased hematopoietic *in vivo* (Figure S8). The hematopoietic maturation step in the
306 presence of OP9-DL1 feeder line unlikely causes T-lineage-biased iHPC, as an

307 inducible expression of another transcription factor cocktails in PSC exactly using the
308 same protocol giving rise to iHPC preferentially contributing to B lymphopoiesis in B-
309 NDG recipients (unpublished data). Nonetheless, our data support the concept that
310 synergies of distinct transcription factors intrinsically determine variable hematopoietic
311 lineage potentials at as early as hemogenic endothelial cell phase.

312 Intravenous infusion of the iHPC from *iR9*-PSC successfully reconstituted iT
313 lymphopoiesis *in vivo*. The induced LSK cells from the primary iHPC recipients further
314 gave rise to T lymphocytes in secondary recipients. The occurrences of iDN1, iDN2,
315 iDN3, iDN4 cells at different time-points in the thymi of iT-B-NDG mice strongly
316 indicated that the induced pre-thymic progenitors ($Lin^{-}c\text{-}kit^{+}CD127^{+}/CD135^{+}$) have the
317 capacities of homing to central lymphoid organs and developed normally following a
318 cellular trajectory resembling natural T cell development. Besides the pivotal roles of
319 exogenous *Runx1* and *Hoxa9* during EHT and subsequent iHPC maturation phases, we
320 could not exclude the possibilities that the weak leaky expression of these two factors
321 further facilitated the iT cell development *in vivo* after infusion into immune-deficient
322 mice, as *Runx1* and *Hoxa9* are also involved in T cell development in bone marrow (*67*)
323 and thymus (*21*). In contrast to our approach, an induced T cell progenitor population
324 (DN2/DN3 cell phase) from mouse ESC lacked thymus-homing capacity *in vivo* and
325 required congenic fetal thymus organ for further development into mature T cells (*11*),
326 which implicated that an intrinsic gene network program essential for physiological T
327 cell development were not fully activated during hematopoietic induction from PSC,
328 which can be rescued by exogenous expression of *Runx1* and *Hoxa9*. Nonetheless, our

329 approach fully reconstitutes functional T lymphopoiesis *in vivo* using PSC source,
330 which avoids the malfunction risks of *in vitro* generated T cells due to the insufficiency
331 of negative and positive selections.

332 The single iHEC exhibited a transcriptome signature resembling E11 AGM EC and
333 pre-HSC. Activating the signature genes lacking in the iHEC but abundant in natural
334 E11 AGM EC or pre-HSC might further promote the production of a homogenous
335 iHEC population, thus consequently resulting in more efficient T cell generation or
336 multi-lineage hematopoietic. The feature of T cell-lineage-bias commitment from *iR9*-
337 PSC brings advantages for gene editing using *iR9*-PSC rather than using canonical adult
338 HSPC, since manipulating HSPC *in vitro* always faces stemness loss and might even
339 introduce unknown impacts on the functions of other blood lineage derivatives from
340 the edited HSPC.

341 In conclusion, this study establishes a novel approach of preferentially reconstituting
342 functional and therapeutic T lymphopoiesis *in vivo* using PSC source by defined
343 transcription factors. At single cell resolution, we unveil that the T-lineage specification
344 is determined at as early as hemogenic endothelial cell stage and identify the *bona fide*
345 pre-thymic progenitors with thymus-homing features. This study provides insight into
346 therapeutic T cell generation in vivo using PSC source, which is promising for PSC-
347 based universal and personalized immunotherapy.

348 **ACKNOWLEDGEMENTS**

349 This work is supported by the Strategic Priority Research Program of Chinese Academy
350 of Sciences (XDA16010208), the Major Research and Development Project of

Guangzhou Regenerative Medicine and Health Guangdong Laboratory (2018GZR110104006), the CAS Key Research Program of Frontier Sciences (QYZDB-SSW-SMC057), the Chinese Ministry of Science and Technology (2015CB964401, 2016YFA0100601, 2017YFA0103401, 2015CB964902, and 2015CB964901), the Health and Medical Care Collaborative Innovation Program of Guangzhou Scientific and Technology (201803040017), the Major Scientific and Technological Project of Guangdong Province (2014B020225005), the Science and Technology Planning Project of Guangdong Province (2017B030314056), the Program for Guangdong Introducing Innovative and Entrepreneurial Teams (2017ZT07S347), the National Natural Science Foundation of China (31471117, 81470281, 31600948, 31425012).

AUTHOR CONTRIBUTIONS

R.G. and F.H. conducted all the major experiments, data analysis and wrote the manuscript. Q.W., C.Lv, H.W., L.L., Y.Z., Z.B., M.Z., Y.L., X.L., C.X., T.W., P.Z., K.W., Y.D., Y.L., YX.G. and Y.G. participated in multiple experiments; Q.W. and Z.L. performed RNA-Seq and data analysis. C.Lv, H.W., Y.L., P.Z., Y.L., X.Z. and J.C. constructed vectors, prepared iPSC, designed and participated gene editing. Y.L. and YQ.L. discussed the single cell data; B.L. and J.W. discussed the data and wrote the manuscript; and J.W. designed the project and provided the final approval of the manuscript.

DECLARATION OF INTERESTS

The authors declare no competing interests.

MATERIALS AND METHODS

MICE

B-NDG (NOD-*Prkdc*^{Scid}*IL2rg*^{tm1}/Bcgen, CD45.1^{+}) mice were purchased from Biocytogen Jiangsu Co., Ltd (Jiangsu, China). BALB/c and C57BL/6 (CD45.2^{+}) mice were purchased from Bejing Vital River Laboratory Animal Technology. *Rag1*$^{-/-}$ mice (C57BL/6 background) were a gift from Dr. Z. Liu from Institute of Biophysics (CAS, China). Mice were housed in the SPF-grade animal facility of the Guangzhou Institutes of Biomedicine and Health, Chinese Academy of Sciences (GIBH, CAS, China). All animal experiments were approved by the Institutional Animal Care and Use Committee of Guangzhou Institutes of Biomedicine and Health (IACUC-GIBH).

CELL CULTURE

Mouse embryonic fibroblasts (MEFs) were derived from 13.5 d.p.c C57BL/6 mouse embryos. MEFs were maintained in DMEM/high glucose (Hyclone), 10% FBS (Natocor) supplemented with 1% nonessential amino acids (NEAA, Gibco). C57BL/6 mouse embryonic stem cells (Biocytogen) were maintained on feeder layers in ES medium containing DMEM/high glucose, 15% FBS (Gibco), 1% NEAA, 1% GlutaMAX (Gibco), 1% Sodium Pyruvate (Gibco), 0.1 mM β-mercaptoethanol (Gibco), 1 μM PD0325901 (Selleck), 3 μM Chir99021 (Selleck) and 1000 U/ml LIF. The OP9-DL1 cells (GFP^{+}) were maintained in α-MEM (Gibco) supplemented with 20% FBS (CellMax). The AFT024 cell lines (ATCC) were maintained in DMEM/high glucose, 10% FBS (Natocor) supplemented with 0.1 mM β-mercaptoethanol and 1% Sodium

Pyruvate. HEK293T (ATCC) and Plat-E (Cell Biolabs, Inc) cells were maintained in DMEM/high glucose supplemented with 10% FBS (Natocor). Ka539 B cell lymphoma cell line (C57BL/6 background) was a gift from Chong Chen lab (Sichuan University). Ka539 cells transfected with a virus expressing luciferase reporter were cultured in DMEM/high glucose and IMDM (Gibco) supplemented with 10% FBS (Natocor), 0.1 mM β-mercaptoethanol. E.G7-OVA cell line (ATCC) was cultured in RPMI 1640 (Gibco) supplemented with 10% FBS (Natocor), 1% GlutaMAX, 1% sodium pyruvate, and 0.1 mM β-mercaptoethanol.

HEMATOPOIETIC DIFFERENTISTION

PSC were trypsinized by 0.05% Trypsin-EDTA (Gibco) and resuspended in the basic differentiation medium (BDM: IMDM, 15% FBS (Gibco), 200μg/ml iron-saturated transferring (Sigma), 0.45 mM monothiolglycerol (Sigma), 1% GlutaMAX, and 50 μg/ml ascorbic acid (Sigma)). For removing the feeder layers, the PSC were plated into the 0.1% gelatin-coated (Merck Millipore) well, and the floating cells were collected after 40 min. For EB generation (*68*), the PSC were resuspended at 100,000 cells/ml in the BDM supplemented with 5 ng/ml BMP4 (Peprotech) and plated at 20 ul/drop for inverted culture in 15 cm dishes. At day 2.5, EBs were replanted into gelatinized plates in BDM supplemented with 5 ng/ml BMP4 and 5 ng/ml VEGF (Peprotech). At day 6, the medium was changed to BDM supplemented with 2% conditioned medium derived from the supernatants of AFT024-mIL3, AFT024-mIL6, AFT024-hFlt3L and AFT024-mSCF cell culture. Doxycycline (1 μg/ml, Sigma) was added at day 6. The medium was replaced every other day. The plates were seeded with OP9-DL1 cells (20000 cells/well,

12-well plate) 12 hours prior to the hematopoietic maturation step in EM medium (α-MEM, 15% DFBS (Hyclone), 200 μg/ml iron-saturated transferring, 0.45 mM monothiolglycerol, 1% GlutaMAX, 50 μg/ml ascorbic acid, 2% conditioned medium derived from supernatants of AFT024-mIL3, AFT024-hFlt3L and AFT024-mSCF cell culture and 1 μg/ml doxycycline. 100-500 sorted iHEC were seeded into each well for hematopoietic maturation. The EM was half-replaced every two days.

TRANSPLANTION OF iHPC

8-10-week-old B-NDG mice were sublethally irradiated (2.25 Gy) by an X-ray irradiator (RS2000, Rad Source Inc.). 0.5-1 million PSC-derived iHPC were injected into each irradiated B-NDG mouse via retro-orbital veins. The mice were fed with water containing co-trimoxazole (Tianjin Lisheng Pharmaceutical co., LTD) for two weeks to prevent infection.

T LYMPHOCYTE INDUCTION *IN VITRO*

For T lymphocyte induction *in vitro*, OP9-DL1 coculture method(*6*) was used with minor modifications. Briefly, the single-cell suspensions of iHPC (Day 21) were maintained on OP9-DL1 feeder cells in T cell induction medium (TIM, α-MEM, 20% DFBS, and 1% GlutaMAX) supplemented with 2% conditioned medium derived from supernatants of AFT024-hFlt3L and AFT024-hIL7 cell culture for sustained 12 days. The iHEC-derived cells were trypsinized into single-cell suspensions and replanted into fresh OP9-DL1 monolayers every 6 days. And the TIM was replaced every 3 days.

GENE EDITING

Mouse MEF cells were reprogrammed into iPSC as described (*69*). The *CAG Pr-rtTA-*

439 *3×Stop-TRE-Runx1-p2a-Hoxa9-pA-PGK Pr-HygroR* cassette was inserted into the
440 *Rosa26 locus* of mouse ESC/iPSC. The positive clones (*iR9*-ESC/iPSC) were selected
441 by Hygromycin B (150 μg/ml, Invivogen) were further cultured in ES medium
442 supplemented with Dox (1 μg/ml). The induced expression of *Runx1* and *Hoxa9* was
443 confirmed by qPCR. For the generation of *OT1-iR9*-iPSC, a *CAG Pr-OT1 TCRα-p2a-*
444 *TCRβ-IRES-GFP-PGK Pr-PuroR* cassette was inserted into the *Hipp11 locus* of *iR9-*
445 iPSC. The *OT1* sequence was cloned from murine TCR OT1-2A.pMIG II (Addgene).
446 The *OT1-iR9*-iPSC positive clones were further selected by Puromycin (1 μg/ml,
447 Invivogen) and the expression of OT1-TCR were measured by intra-cellular staining.

448 **FLOW CYTOMETRY AND CELL SORTING**

449 Single-cell suspensions were prepared by 0.05% Trypsin-EDTA and filtered by 70 μm
450 filter. Single cells were blocked by Fc (CD16/32) (93, eBioscience) antibody, and then
451 stained with related antibodies. The following antibodies were used: c-kit (2B8,
452 eBioscience), CD31 (390, eBioscience), CD41 (eBioMWReg30, eBioscience), CD45
453 (30-F11, eBioscience), CD45.1 (A20, eBioscience), CD45.2 (104, eBioscience), CD2
454 (RM2-5, eBioscience), CD3 (145-2C11, eBioscience), CD4 (GK1.5, eBioscience),
455 CD8a (53-6.7, eBioscience), CD19(eBio1D3, eBioscience), B220 (RA3-6B2,
456 eBioscience), CD11b (M1/70, eBioscience), NK1.1 (PK136, eBioscience), Ter119
457 (TER-119, eBioscience), Gr1 (RB6-8C5, eBioscience), CD201 (eBio1560,
458 eBioscience), CD135 (A2F10, eBioscience), CD127 (A7R34 eBioscience) FcεRIα
459 (MAR-1, biolegend), CD69 (H1.2F3, biolegend), CD62L (MEL-14, biolegend) IFNγ
460 (XMG1.2, biolegend), IL17 (TC11-18H10.1, biolegend), CD44 (IM7, eBioscience),

CD25 (PC61.5, eBioscience), TCRβ (H57-597, eBioscience), TCRγδ (GL3, eBioscience), TCRvα2 (B20.1, biolegend), TCRvβ5.1/5.2 (MR9-4, biolegend) Streptavidin PE-Cy7 (eBioscience), Streptavidin eFlour 450 (eBioscience), Streptavidin PE-Cy5 (biolegend). The cells were resuspended in the DAPI solution, or PI solution (eBioscience) and were analyzed with Fortessa cytometer (BD Biosciences). The cells were sorted using Arial II cytometer (BD Biosciences). The flow data were analyzed with FlowJo (Three Star, Ashland OR).

ALLOGENEIC SKIN TRANSPLANTION

Individual *Rag1*$^{-/-}$ mice (8-10 weeks old) were adoptively transferred with splenic cells equivalent to 5 million CD4^{+} and CD8^{+} iT cells from iT-B-NDG mice. Four days after iT cell transfer, the allogeneic skin (BALB/c background) was transplanted as described (*70*). Grafts were considered rejection if there was a loss of distinct border, visible signs of ulceration and necrosis to 80% of the graft area. The rejected skin tissues were removed for analysis 9 days after skin transplantation. For analysis activated iT cells in rejected skin grafts, the single cell suspensions were prepared as described (*71*). The activated alloreactive iT lymphocytes were defined as CD45.2^{+}Ter119^{-}CD11b^{-} CD69^{+}CD44^{+}CD4^{+}/CD8^{+}. For analysis of cytokines released by the alloreactive iT cells, we used anti-IL17 and anti-IFNγ antibodies following an intracellular staining protocol (eBioscience).

OT1-iT ANTI-TUMOR ASSAY

For the reconstitution of the OT1-iT cells in *Rag1*$^{-/-}$ mice, three million OT1-iHPC were transplanted into each irradiated *Rag1*$^{-/-}$ mouse (4.5 Gy). OT1-iT cells (GFP^{+} CD8^{+}

TCRVβ5$^+$ TCRVα2$^+$) in PB were analyzed six weeks post-transplantation. The E.G7-OVA cells were transplanted into the groin of the OT1-iT reconstituted mice by subcutaneous injection (0.2 million/mouse). The tumor size was measured every 2 days and was calculated as length × width (mm^2). Mice with tumor size larger than 20 mm at the longest axis were euthanized for ethical consideration. To analyze the tumor-infiltrating OT1-iT cells, tumors were isolated at day 15 and digested for 30 min at 37 ℃ by collagen IV solution (1mg/ml, Gibco) after being cut up. Then, the single-cell suspensions were harvested for staining. The activated iT cells were defined as CD45.2$^+$GFP$^+$CD8$^+$CD44$^+$CD62L$^-$.

RNA-SEQ AND DATA ANALYSIS

The cDNA of single iHEC sorted on day 11, and iHPC at Day 14, 17, and 21 or 1,000-CD4SP/CD8SP iT-cell aliquots of from spleens of iT-B-NDG mice were generated and amplified using Discover-sc WTA Kit V2 (Vazyme). The quality of amplified cDNA was assessed by qPCR analysis of housekeeping genes (B2m and Gapdh). Samples that passed quality control were used for sequencing library preparation by TruePrep DNA Library Prep Kit V2 (Vazyme). All libraries were sequenced by illumina sequencer NextSeq 500. The raw data (fastq files) were generated using bcl2fastq software (version 2.16.0.10) and were uploaded to the Gene Expression Omnibus public database (GSE121371, GSE121373, GSE128738). The raw reads were aligned to mouse genome mm10 by HISAT2 (version 2.1.0) (*72*) and the expression levels in TPM were estimated by StringTie (version 1.3.4) (*73, 74*). The wildtype CD4SP T cells, CD8SP T cells, myeloid cells, and B cells sequencing data (GSE105057) were

505 downloaded from Gene Expression Omnibus (*75*). Heat maps were plotted using
506 pheatmap (version 1.0.8). The natural embryonic single-cell data (endothelial cells
507 ($CD31^+$VE-cadherin$^+CD41^-CD43^-CD45^-Ter119^-$) and pre-HSCs ($CD31^+CD45^-$
508 $CD41^{low}$c-kit^+CD201^{high}) were downloaded from Gene Expression Omnibus
509 (GSE67120) (*22*). The batch effects of single-cell data between iHEC and natural
510 embryonic cells were removed using ComBat (sva R package, version 3.26.0). The
511 prcomp function of stats (R package, version 3.4.4) was used for PCA. The DESeq2
512 was used for differential expression analysis. The PCA plot and violin plot were plotted
513 using ggplot2 (R package, version 2.2.1). tSNE was performed by Rtsne (R package
514 version 0.15). The TPM values of transcription factors were log2-converted.

515 For TCRαβ sequencing, 15,000 sorted CD4SP, and CD8SP naïve iT cells were sorted
516 from thymus or spleen of iT-B-NDG mice. The sorted iT cells of thymus were gated on
517 $CD45.2^+Ter119^-CD11b^-Gr1^-CD19^-B220^-NK1.1^-TCR\gamma\delta^-CD4^+CD8^-$ and
518 $CD45.2^+Ter119^-CD11b^-Gr1^-CD19^-B220^-NK1.1^-TCR\gamma\delta^-CD4^-CD8^+$. The splenic naïve
519 iT cells were gated on $CD45.2^+CD4^+CD8^-CD62L^+CD44^-$ and $CD45.2^+CD4^-$
520 $CD8^+CD62L^+CD44^-$. The cDNA was generated and amplified by SMARTer Mouse
521 TCRαβ Profiling Kit (Clontech). Libraries were sequenced by illumina sequencer
522 MiSeq (2×250 cycles). The raw data (fastq files) were generated using illumina
523 bcl2fastq software and were uploaded to Gene Expression Omnibus public database
524 (GSE121374). T cell receptors αβ chains repertoires were aligned and assembled using
525 software MiXCR (version 2.1.12) (*48*). The TCRαβ clonotypes were exported
526 respectively by parameter '--chains' in exportClones command of MiXCR. The

exported clonotypes were visualized in the form of chord diagram using VDJtools software (version 1.1.10) (*76*).

STATISTICS

All quantitative analyses were based on a minimum of at least three sample replicates. Data are presented as means ± s.d. by GraphPad Prism. Independent-sample student T test and One-way ANOVA were performed (SPSS). NS, no significance; *p < 0.05; **p < 0.01; ***p < 0.001.

REFERENCES

1. G. Gross, G. Gorochov, T. Waks, Z. Eshhar, Generation of effector T cells expressing chimeric T cell receptor with antibody type-specificity. *Transplant Proc* **21**, 127-130 (1989).
2. R. A. Morgan *et al.*, Cancer regression in patients after transfer of genetically engineered lymphocytes. *Science* **314**, 126-129 (2006).
3. J. Hartmann, M. Schussler-Lenz, A. Bondanza, C. J. Buchholz, Clinical development of CAR T cells-challenges and opportunities in translating innovative treatment concepts. *EMBO Mol Med* **9**, 1183-1197 (2017).
4. M. Sadelain, I. Riviere, S. Riddell, Therapeutic T cell engineering. *Nature* **545**, 423-431 (2017).
5. K. Takahashi, S. Yamanaka, Induction of pluripotent stem cells from mouse embryonic and adult fibroblast cultures by defined factors. *Cell* **126**, 663-676 (2006).
6. T. M. Schmitt, J. C. Zuniga-Pflucker, Induction of T cell development from hematopoietic progenitor cells by delta-like-1 in vitro. *Immunity* **17**, 749-756 (2002).
7. M. Mohtashami *et al.*, Direct comparison of Dll1- and Dll4-mediated Notch activation levels shows differential lymphomyeloid lineage commitment outcomes. *J Immunol* **185**, 867-876 (2010).
8. A. Montel-Hagen *et al.*, Organoid-Induced Differentiation of Conventional T Cells from Human Pluripotent Stem Cells. *Cell Stem Cell* **24**, 376-389 e378 (2019).
9. G. Awong *et al.*, Human proT-cells generated in vitro facilitate hematopoietic stem cell-derived T-lymphopoiesis in vivo and restore thymic architecture. *Blood* **122**, 4210-4219 (2013).
10. S. Shukla *et al.*, Progenitor T-cell differentiation from hematopoietic stem cells using Delta-like-4 and VCAM-1. *Nat Methods* **14**, 531-538 (2017).
11. T. M. Schmitt *et al.*, Induction of T cell development and establishment of T cell competence from embryonic stem cells differentiated in vitro. *Nat Immunol* **5**, 410-417 (2004).
12. V. M. Sandler *et al.*, Reprogramming human endothelial cells to haematopoietic cells requires vascular induction. *Nature* **511**, 312-318 (2014).
13. R. Sugimura *et al.*, Haematopoietic stem and progenitor cells from human pluripotent stem

cells. *Nature* **545**, 432-438 (2017).

14. J. Riddell *et al.*, Reprogramming committed murine blood cells to induced hematopoietic stem cells with defined factors. *Cell* **157**, 549-564 (2014).
15. R. Lis *et al.*, Conversion of adult endothelium to immunocompetent haematopoietic stem cells. *Nature* **545**, 439-445 (2017).
16. G. Stik, T. Graf, Hoxb5, a Trojan horse to generate T cells. *Nat Immunol* **19**, 210-212 (2018).
17. E. Dzierzak, A. Bigas, Blood Development: Hematopoietic Stem Cell Dependence and Independence. *Cell Stem Cell* **22**, 639-651 (2018).
18. M. Yoshimoto *et al.*, Autonomous murine T-cell progenitor production in the extra-embryonic yolk sac before HSC emergence. *Blood* **119**, 5706-5714 (2012).
19. T. C. Luis *et al.*, Initial seeding of the embryonic thymus by immune-restricted lympho-myeloid progenitors. *Nat Immunol* **17**, 1424-1435 (2016).
20. Y. Tian *et al.*, The first wave of T lymphopoiesis in zebrafish arises from aorta endothelium independent of hematopoietic stem cells. *J Exp Med* **214**, 3347-3360 (2017).
21. M. A. Yui, E. V. Rothenberg, Developmental gene networks: a triathlon on the course to T cell identity. *Nat Rev Immunol* **14**, 529-545 (2014).
22. F. Zhou *et al.*, Tracing haematopoietic stem cell formation at single-cell resolution. *Nature* **533**, 487-492 (2016).
23. P. Sroczynska, C. Lancrin, V. Kouskoff, G. Lacaud, The differential activities of Runx1 promoters define milestones during embryonic hematopoiesis. *Blood* **114**, 5279-5289 (2009).
24. M. J. Chen, T. Yokomizo, B. M. Zeigler, E. Dzierzak, N. A. Speck, Runx1 is required for the endothelial to haematopoietic cell transition but not thereafter. *Nature* **457**, 887-891 (2009).
25. T. E. North *et al.*, Runx1 expression marks long-term repopulating hematopoietic stem cells in the midgestation mouse embryo. *Immunity* **16**, 661-672 (2002).
26. Q. Wang *et al.*, Disruption of the Cbfa2 gene causes necrosis and hemorrhaging in the central nervous system and blocks definitive hematopoiesis. *Proc Natl Acad Sci U S A* **93**, 3444-3449 (1996).
27. T. Okuda, J. van Deursen, S. W. Hiebert, G. Grosveld, J. R. Downing, AML1, the target of multiple chromosomal translocations in human leukemia, is essential for normal fetal liver hematopoiesis. *Cell* **84**, 321-330 (1996).
28. H. M. Eilken, S. Nishikawa, T. Schroeder, Continuous single-cell imaging of blood generation from haemogenic endothelium. *Nature* **457**, 896-900 (2009).
29. C. F. Pereira *et al.*, Induction of a hemogenic program in mouse fibroblasts. *Cell Stem Cell* **13**, 205-218 (2013).
30. S. Pearson, S. Cuvertino, M. Fleury, G. Lacaud, V. Kouskoff, In vivo repopulating activity emerges at the onset of hematopoietic specification during embryonic stem cell differentiation. *Stem Cell Reports* **4**, 431-444 (2015).
31. C. W. So, H. Karsunky, P. Wong, I. L. Weissman, M. L. Cleary, Leukemic transformation of hematopoietic progenitors by MLL-GAS7 in the absence of Hoxa7 or Hoxa9. *Blood* **103**, 3192-3199 (2004).
32. V. Ramos-Mejia *et al.*, HOXA9 promotes hematopoietic commitment of human embryonic stem cells. *Blood* **124**, 3065-3075 (2014).
33. M. Magnusson *et al.*, HOXA10 is a critical regulator for hematopoietic stem cells and erythroid/megakaryocyte development. *Blood* **109**, 3687-3696 (2007).

606 34. K. Komorowska *et al.*, Hepatic Leukemia Factor Maintains Quiescence of Hematopoietic Stem
607 Cells and Protects the Stem Cell Pool during Regeneration. *Cell Rep* **21**, 3514-3523 (2017).
608 35. K. L. Davis, Ikaros: master of hematopoiesis, agent of leukemia. *Ther Adv Hematol* **2**, 359-368
609 (2011).
610 36. S. Nagel *et al.*, NKL homeobox gene activities in hematopoietic stem cells, T-cell development
611 and T-cell leukemia. *PLoS One* **12**, e0171164 (2017).
612 37. K. Oakley *et al.*, Setbp1 promotes the self-renewal of murine myeloid progenitors via activation
613 of Hoxa9 and Hoxa10. *Blood* **119**, 6099-6108 (2012).
614 38. E. S. Ng *et al.*, Differentiation of human embryonic stem cells to HOXA(+) hemogenic
615 vasculature that resembles the aorta-gonad-mesonephros. *Nat Biotechnol* **34**, 1168-1179
616 (2016).
617 39. M. A. Inlay *et al.*, Identification of multipotent progenitors that emerge prior to hematopoietic
618 stem cells in embryonic development. *Stem Cell Reports* **2**, 457-472 (2014).
619 40. X. He, K. Park, D. J. Kappes, The role of ThPOK in control of CD4/CD8 lineage commitment. *Annu*
620 *Rev Immunol* **28**, 295-320 (2010).
621 41. K. Germar *et al.*, T-cell factor 1 is a gatekeeper for T-cell specification in response to Notch
622 signaling. *Proc Natl Acad Sci U S A* **108**, 20060-20065 (2011).
623 42. P. Aliahmad, A. Seksenyan, J. Kaye, The many roles of TOX in the immune system. *Curr Opin*
624 *Immunol* **24**, 173-177 (2012).
625 43. E. H. Palacios, A. Weiss, Function of the Src-family kinases, Lck and Fyn, in T-cell development
626 and activation. *Oncogene* **23**, 7990-8000 (2004).
627 44. T. Taghon, M. A. Yui, E. V. Rothenberg, Mast cell lineage diversion of T lineage precursors by the
628 essential T cell transcription factor GATA-3. *Nat Immunol* **8**, 845-855 (2007).
629 45. P. Liu, P. Li, S. Burke, Critical roles of Bcl11b in T-cell development and maintenance of T-cell
630 identity. *Immunol Rev* **238**, 138-149 (2010).
631 46. K. Hahm *et al.*, Helios, a T cell-restricted Ikaros family member that quantitatively associates
632 with Ikaros at centromeric heterochromatin. *Genes Dev* **12**, 782-796 (1998).
633 47. T. Y. Halim *et al.*, Retinoic-acid-receptor-related orphan nuclear receptor alpha is required for
634 natural helper cell development and allergic inflammation. *Immunity* **37**, 463-474 (2012).
635 48. D. A. Bolotin *et al.*, MiXCR: software for comprehensive adaptive immunity profiling. *Nat*
636 *Methods* **12**, 380-381 (2015).
637 49. L. A. Garrett-Sinha, Review of Ets1 structure, function, and roles in immunity. *Cell Mol Life Sci*
638 **70**, 3375-3390 (2013).
639 50. F. Zohren *et al.*, The transcription factor Lyl-1 regulates lymphoid specification and the
640 maintenance of early T lineage progenitors. *Nat Immunol* **13**, 761-769 (2012).
641 51. H. Hock *et al.*, Tel/Etv6 is an essential and selective regulator of adult hematopoietic stem cell
642 survival. *Genes Dev* **18**, 2336-2341 (2004).
643 52. K. T. Greig, S. Carotta, S. L. Nutt, Critical roles for c-Myb in hematopoietic progenitor cells. *Semin*
644 *Immunol* **20**, 247-256 (2008).
645 53. A. C. Wilkinson *et al.*, Single-cell analyses of regulatory network perturbations using enhancer-
646 targeting TALEs suggest novel roles for PU.1 during haematopoietic specification. *Development*
647 **141**, 4018-4030 (2014).
648 54. S. H. M. Pang *et al.*, PU.1 Is Required for the Developmental Progression of Multipotent
649 Progenitors to Common Lymphoid Progenitors. *Front Immunol* **9**, 1264 (2018).

55. R. Sugimura, The significance and application of vascular niche in the development and maintenance of hematopoietic stem cells. *Int J Hematol* **107**, 642-645 (2018).
56. V. Azcoitia, M. Aracil, A. C. Martinez, M. Torres, The homeodomain protein Meis1 is essential for definitive hematopoiesis and vascular patterning in the mouse embryo. *Dev Biol* **280**, 307-320 (2005).
57. C. H. Nam, T. H. Rabbitts, The role of LMO2 in development and in T cell leukemia after chromosomal translocation or retroviral insertion. *Mol Ther* **13**, 15-25 (2006).
58. Y. Yu *et al.*, Bcl11a is essential for lymphoid development and negatively regulates p53. *J Exp Med* **209**, 2467-2483 (2012).
59. D. Boutboul *et al.*, Dominant-negative IKZF1 mutations cause a T, B, and myeloid cell combined immunodeficiency. *J Clin Invest* **128**, 3071-3087 (2018).
60. A. P. Weng *et al.*, c-Myc is an important direct target of Notch1 in T-cell acute lymphoblastic leukemia/lymphoma. *Genes Dev* **20**, 2096-2109 (2006).
61. M. M. Del Real, E. V. Rothenberg, Architecture of a lymphomyeloid developmental switch controlled by PU.1, Notch and Gata3. *Development* **140**, 1207-1219 (2013).
62. S. Uehara *et al.*, Premature expression of chemokine receptor CCR9 impairs T cell development. *J Immunol* **176**, 75-84 (2006).
63. D. A. Zlotoff *et al.*, CCR7 and CCR9 together recruit hematopoietic progenitors to the adult thymus. *Blood* **115**, 1897-1905 (2010).
64. R. Tussiwand *et al.*, The preTCR-dependent DN3 to DP transition requires Notch signaling, is improved by CXCL12 signaling and is inhibited by IL-7 signaling. *Eur J Immunol* **41**, 3371-3380 (2011).
65. M. L. Janas *et al.*, Thymic development beyond beta-selection requires phosphatidylinositol 3-kinase activation by CXCR4. *J Exp Med* **207**, 247-261 (2010).
66. H. J. Lawrence *et al.*, Mice bearing a targeted interruption of the homeobox gene HOXA9 have defects in myeloid, erythroid, and lymphoid hematopoiesis. *Blood* **89**, 1922-1930 (1997).
67. K. A. Gwin, M. B. Shapiro, J. J. Dolence, Z. L. Huang, K. L. Medina, Hoxa9 and Flt3 signaling synergistically regulate an early checkpoint in lymphopoiesis. *J Immunol* **191**, 745-754 (2013).
68. I. Desbaillets, U. Ziegler, P. Groscurth, M. Gassmann, Embryoid bodies: an in vitro model of mouse embryogenesis. *Exp Physiol* **85**, 645-651 (2000).
69. J. Chen *et al.*, Rational optimization of reprogramming culture conditions for the generation of induced pluripotent stem cells with ultra-high efficiency and fast kinetics. *Cell Res* **21**, 884-894 (2011).
70. P. Lan, N. Tonomura, A. Shimizu, S. Wang, Y. G. Yang, Reconstitution of a functional human immune system in immunodeficient mice through combined human fetal thymus/liver and CD34+ cell transplantation. *Blood* **108**, 487-492 (2006).
71. X. Jiang *et al.*, Skin infection generates non-migratory memory CD8+ T(RM) cells providing global skin immunity. *Nature* **483**, 227-231 (2012).
72. D. Kim, B. Langmead, S. L. Salzberg, HISAT: a fast spliced aligner with low memory requirements. *Nat Methods* **12**, 357-360 (2015).
73. M. Pertea *et al.*, StringTie enables improved reconstruction of a transcriptome from RNA-seq reads. *Nat Biotechnol* **33**, 290-295 (2015).
74. M. Pertea, D. Kim, G. M. Pertea, J. T. Leek, S. L. Salzberg, Transcript-level expression analysis of RNA-seq experiments with HISAT, StringTie and Ballgown. *Nat Protoc* **11**, 1650-1667 (2016).

694 75. M. Zhang *et al.*, Transcription factor Hoxb5 reprograms B cells into functional T lymphocytes.
695 *Nat Immunol* **19**, 279-290 (2018).
696 76. M. Shugay *et al.*, VDJtools: Unifying Post-analysis of T Cell Receptor Repertoires. *PLoS Comput*
697 *Biol* **11**, e1004503 (2015).

698

699

FIGURES AND FIGURE LEGENDS

Figure 1

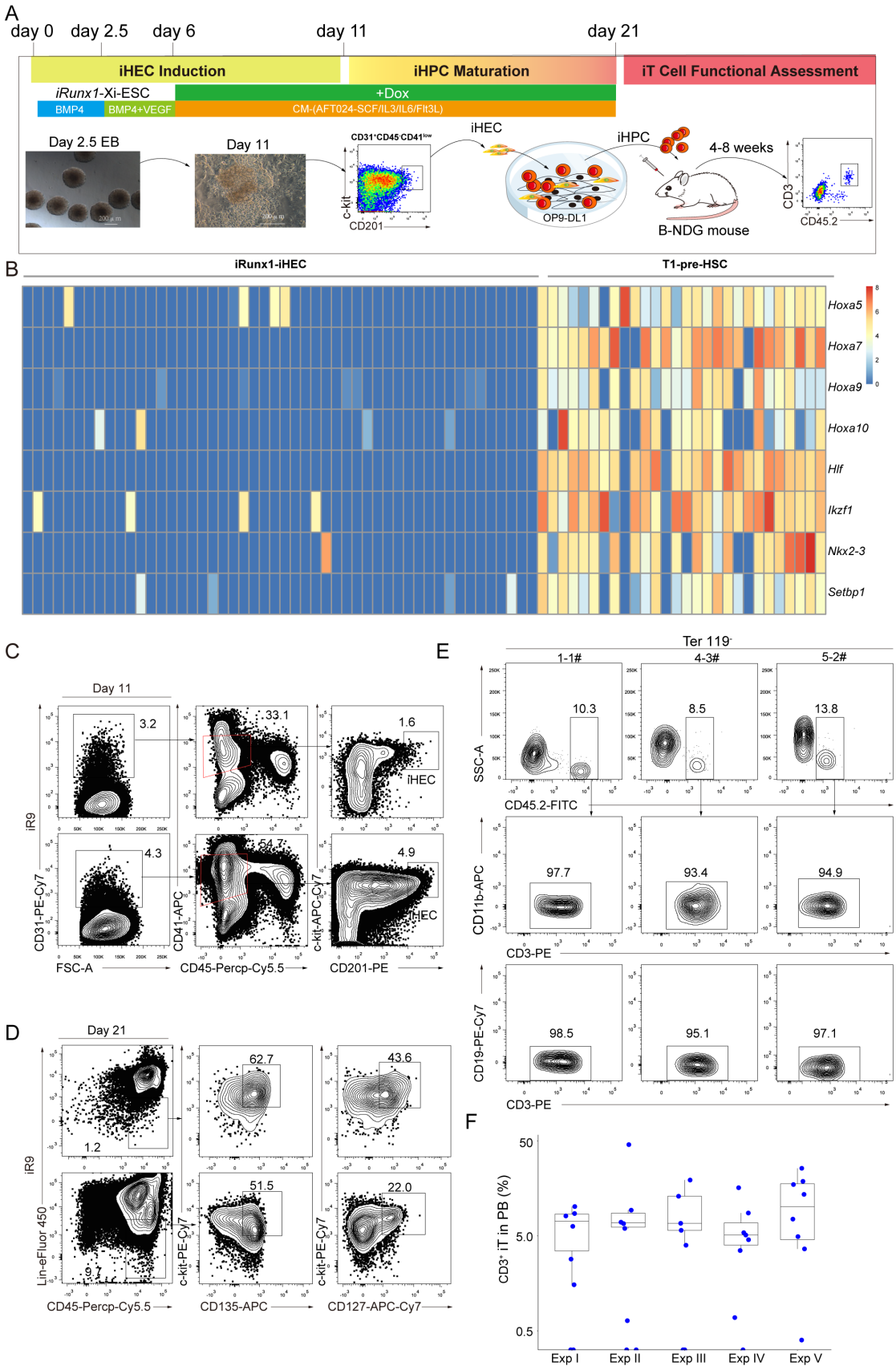

Figure 1. T Cell Regeneration *in vivo* from *iRunx1-p2a-Hoxa9*-edited Embryonic Stem Cells

(A) The strategy of stepwise T lineage induction by defined transcription factors. iRunx1-ESC, and iRunx1-Xi- ESC lines (C57BL/6 background, CD45.2 strain) were used for T cell lineage induction. Xi means one of the eight transcription factors *Hoxa5*, *Hoxa7*, *Hoxa9*, *Hoxa10*, *Hlf*, *Ikzf1*, *Nkx2-3*, *Setbp1*. For EB generation, each of the gene-edited ESC lines was resuspended at 100000 cells/ml in basic differentiation medium (BDM) supplemented with 5ng/ml BMP4 and plated at 20 ul/drop in inverted 15 cm dishes. At day 2.5, EBs were replanted into gelatinized plates in BDM supplemented with 5 ng/ml BMP4 and 5 ng/ml VEGF. At day 6, the medium was changed to BDM supplemented with 2% conditioned medium derived from the supernatants of AFT024-mIL3, AFT024-mIL6, AFT024-hFlt3L and AFT024-mSCF cell culture. Doxycycline (1 μg/ml) was added at day 6. Induced hemogenic endothelial progenitors (iHEC) were defined as $CD31^{+}CD41^{low}CD45^{-}c\text{-}kit^{+}CD201^{high}$. For maturation step, the plates were pre-seeded with OP9-DL1 cells (20000 cells/well, 12-well plate) 12 hours prior maturation in EM medium (α-MEM, 15% DFBS, 200 μg/ml iron-saturated transferring, 0.45 mM monothiolglycerol, 1% glutaMAX, 50 μg/ml ascorbic acid, 2% conditioned medium derived from supernatants of AFT024-mIL3, AFT024-hFlt3L and AFT024-mSCF cell culture, and 1 μg/ml doxycycline. 100-500 sorted iHEC were plated into each well for maturation. The EM was half-replaced every two days. After maturation, the bulk blood cells were assessed for T lineage generation potential.

(B) Heatmaps of the eight transcription factors abundantly expressed in embryonic pre-HSC but rarely expressed in iRunx1-ES derived iHEC. The expression value (TPM) of each gene was converted by log2 and illustrated by pheatmap (R package). One column represents one cell repeat. (iRunx1-iHEC, n=50 single cells, T1-pre-HSC, n=28 single cells).

(C) Sorting gates of iHEC population at day 11 derived from *iRunx1-Hoxa9*-ES line (*iR9*-ESC). Two representative plots from five independent experiments are shown.

(D) Immuno-phenotypes of pre-thymic progenitors in induced hematopoietic progenitor cells from iHEC after ten-day maturation. Two representative plots from five independent experiments. Lin was defined as $CD2^-CD3^-CD4^-CD8^-CD11b^-Gr1^-Ter119^-CD19^-NK1.1^-TCR\gamma\delta^-$. Pre-thymic progenitors were defined as $Lin^-c\text{-}kit^+CD127^+/CD135^+$.

(E) Pluripotent stem cell-derived T cells in PB of B-NDG mice were analyzed by flow cytometry 4 weeks after transplantation. One million iHEC-derived hematopoietic cells were transplanted into individual B-NDG mice ($CD45.1^+$) irradiated by X-ray (2.25 Gy). Three representative mice from five independent experiments were analyzed.

(F) Summary of pluripotent stem cell-derived T cells in PB of individual B-NDG mice from five independent experiments. Forty B-NDG mice transplanted with ESC-derived iHPC were analyzed. The box plot shows the percentage of the $CD3^+$ iT cells in PB, the percentage values were illustrated by ggplot2 (R package). A base-10 logarithmic scale was used for the Y-axis. One point represents one mouse.

Figure 2

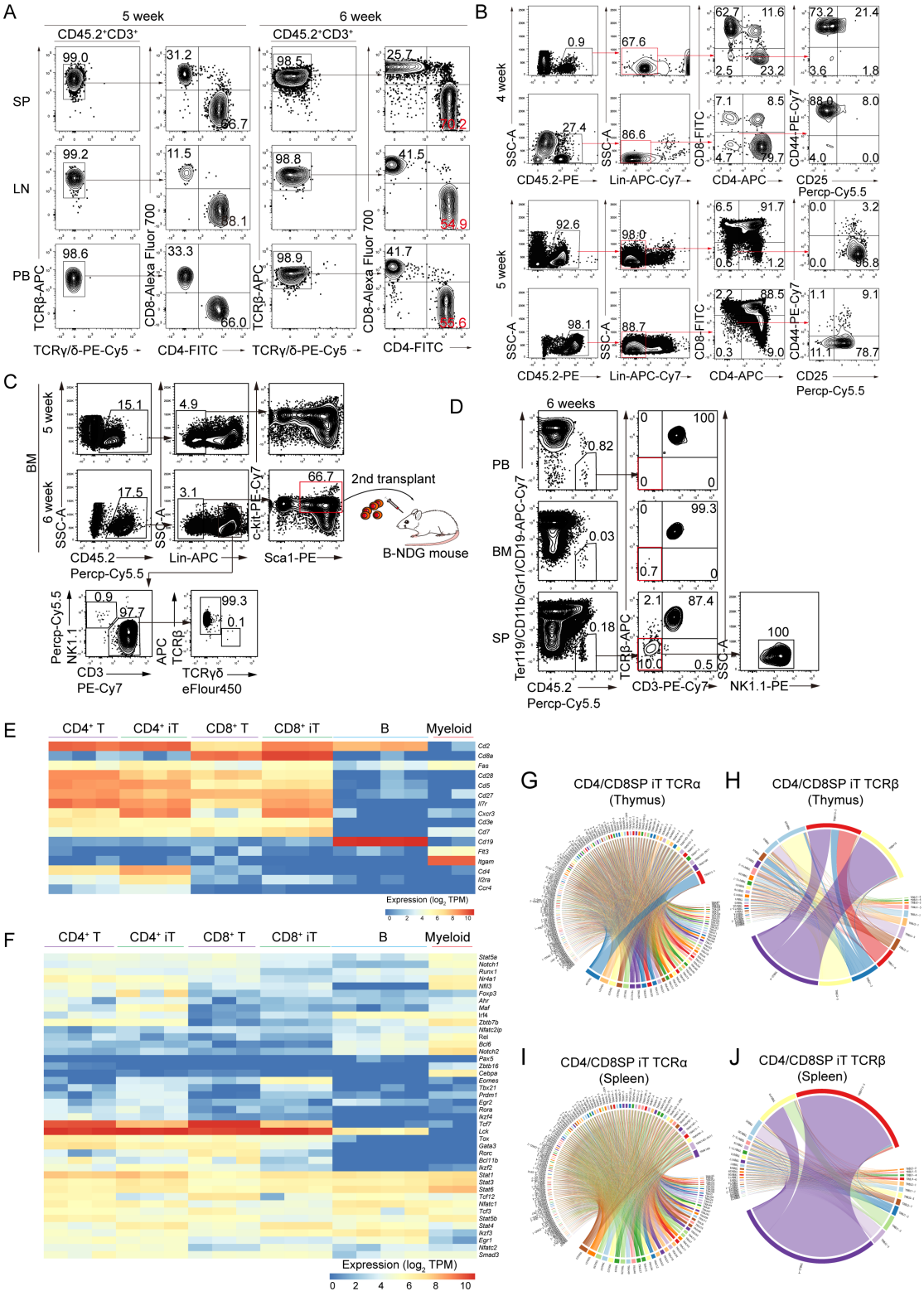

Figure 2. Tissue Distributions, Transcriptome Characterization, and TCRα/β Diversities of ESC-derived T Cells

(A) Flow cytometry analysis of mature iT cells in spleen (SP), lymph node (LN), and

peripheral blood (PB) of B-NDG mice transplanted with ESC-derived hematopoietic cells. Each B-NDG mouse was transplanted with one million iHPC collected on day 21. Representative mouse was sacrificed and analyzed at 5 and 6 weeks after transplantation. Data from two representative mice are shown.

(B) Flow cytometry analysis of iDN cells in the thymus of B-NDG mice transplanted with ESC-derived hematopoietic cells. Each B-NDG mouse was transplanted with one million iHPC at day 21. Representative mouse was sacrificed and analyzed at 4 and 5 weeks after transplantation. Data from four representative mice of two independent experiments are shown. Lin was defined as $Ter119^{-}CD11b^{-}Gr1^{-}CD19^{-}B220^{-}NK1.1^{-}TCR\gamma\delta^{-}$.

(C) Flow cytometry analysis of iHPC in bone marrow (BM) transplanted with iHPC. Each B-NDG mouse was transplanted with one million iHPC collected at day 10 in the presence of OP9-DL1 feeder cells. Representative mouse was sacrificed and analyzed 5 weeks and 6 weeks after transplantation. The BM-derived iHPC ($CD45.2^{+}Lin^{-}c\text{-}kit^{mid}Sca1^{+}$) were sorted for 2nd transplantation. Data from two mice are shown.

(D) Flow cytometry analysis of iT and iNK in PB, spleen (SP) and bone marrow (BM) 6 weeks after 2nd transplantation. 500 LSK cells from primary iT mice were used as input for secondary transplantation. The secondary recipients were sacrificed and analyzed 6 weeks after transplantation. Data from one mouse are shown.

(E) Characterization of surface markers on CD4SP and CD8SP iT cells. CD4SP and CD8SP iT cells were sorted from the spleens of B-NDG mice transplanted with ESC derived hematopoietic cells at week-5. One thousand sorted CD4SP or CD8SP iT cells

were used as cell input for each RNA-Seq cell sample. Wild type CD4SP cells and CD8SP cells were sorted from the spleen of wild type mouse (CD45.2, C57BL/6). Wild type B cells and myeloid cells were sorted from the bone marrow of wild type mouse (CD45.2, C57BL/6). The RNA-Seq raw data were aligned to the mouse genome mm10 (hisat2 linux version 2.1.0), and normalized (Stringtie, linux version 1.3.4). The gene expression values (TPM) were log2 converted and further presented as heatmaps (pheatmap 1.0.8 R package). One biological replicate per column. Myeloid cells (n = 2 sample repeats): $Ter119^{-}CD3^{-}CD19^{-}CD11b^{+}$; B cells (n = 4 sample repeats): $Ter119^{-}CD11b^{-}CD3^{-}CD19^{+}$; $CD4^{+}$ cells (n = 3 sample repeats): $Ter119^{-}CD19^{-}CD11b^{-}CD4^{+}$; $CD8^{+}$ cells (n = 3 sample repeats): $Ter119^{-}CD19^{-}CD11b^{-}CD8^{+}$ $iCD4^{+}$ cells (n = 3 sample repeats): $CD45.2^{+}Ter119^{-}CD19^{-}CD11b^{-}CD4^{+}$; $iCD8^{+}$ cells (n = 3 sample repeats): $CD45.2^{+}Ter119^{-}CD19^{-}CD11b^{-}CD8^{+}$.

(F) Characterization of transcription factors in CD4SP and CD8SP iT cells. e, Chord diagram of TCRα diversity in thymus iT cells.

(G) Chord diagram of TCRβ diversity in thymus iT cells.

(H) Chord diagram of TCRα diversity in thymus iT cells.

(I) Chord diagram of TCRβ diversity in spleen iT cells.

(J) Clonotype counts of TCRαβ in iT cells. Aliquots of sorted 15,000 naïve CD4SP and CD8SP iT cells from either thymus or spleen of iT-B-NDG mice were used as cell inputs for TCRαβ sequencing. The TCRαβ cDNA was amplified by SMARTer Mouse TCR a/b Profiling Kit and sequenced by MiSeq (illumina). The fastq raw data were processed by MiXCR and illustrated by VDJtools.

Figure 3

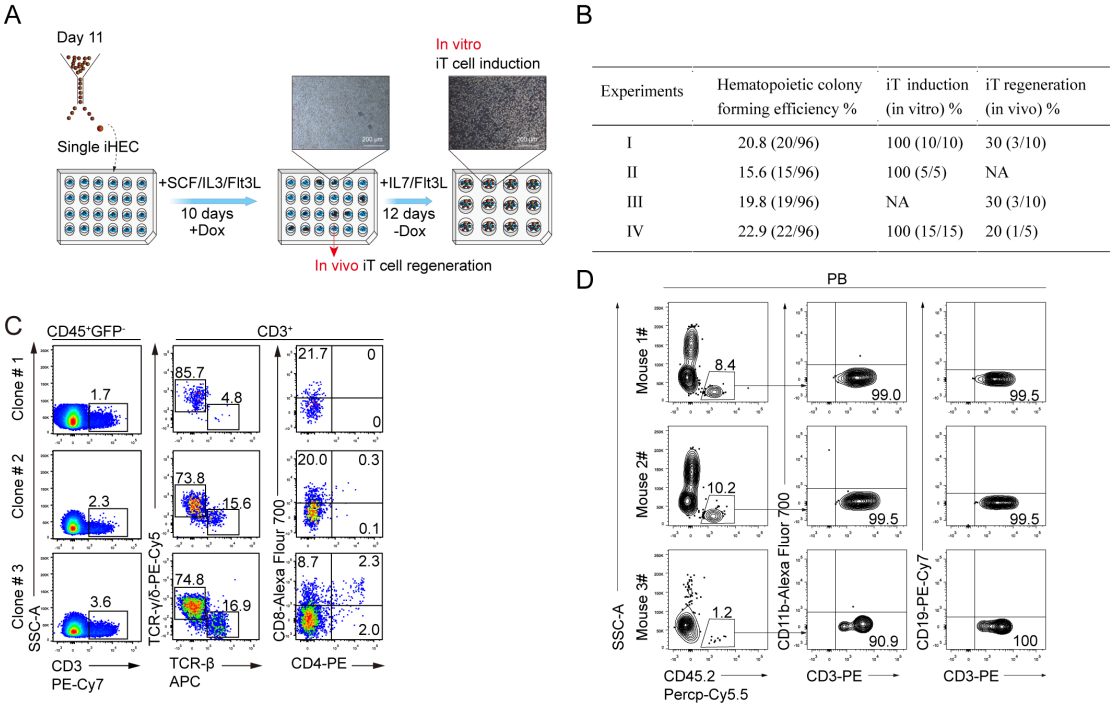

793

794 **Figure 3. Assessment of T Potential of Single iHEC from *iR9*-ESC**

795 (A) The strategy of T cell induction from *iR9*-ESC-derived single iHEC. Single iHEC

796 were sorted into individual wells (24-well plates) pre-seeded with OP9-DL1 feeder cells

797 (10000 cells/well) 12 hours prior maturation in EM medium with doxycycline (1 μg/ml).

798 Doxycycline was sustained for 10 days during the maturation step. After maturation,

799 the bulk blood cells were assessed for T lineage generation potential. For in vivo T cell

800 regeneration, the single iHEC-derived bulk hematopoietic cells (day 10) were

801 transplanted into individual B-NDG recipients. For in vitro T cell induction, the

802 medium was changed to T cell induction medium (TIM, α-MEM, 20% DFBS, and 1%

803 glutaMAX) supplemented with 2% conditioned medium derived from supernatants of

804 AFT024-hFlt3L and AFT024-hIL7 cell culture for sustaining 10 days.

805 (B) Single iHEC efficiently gave rise to T cells. Three hundred and eighty-four single-

806 iHEC at Day 11 were sorted into individual wells (24 well plates). Thirty single-iHEC-

807 formed blood colonies were induced for T cell generation *in vitro*. Cell collections of
808 Twenty-five single-iHEC-formed blood colonies were transplanted into 25 individual
809 B-NDG mice for the assessment of T lymphopoiesis *in vivo*.
810 (C) Flow cytometry analysis of induced T cells from in vitro induction of single iHEC.
811 iT cells from single iHEC culture product (day 22) were analyzed. Plots of iT cells
812 induced from one representative colony are shown.
813 (D) Single iHEC-derived hematopoietic cells gave rise to mature iT cells in PB of B-
814 NDG recipient mice 4 weeks after transplantation. Plots of one representative mouse
815 are shown.

Figure 4

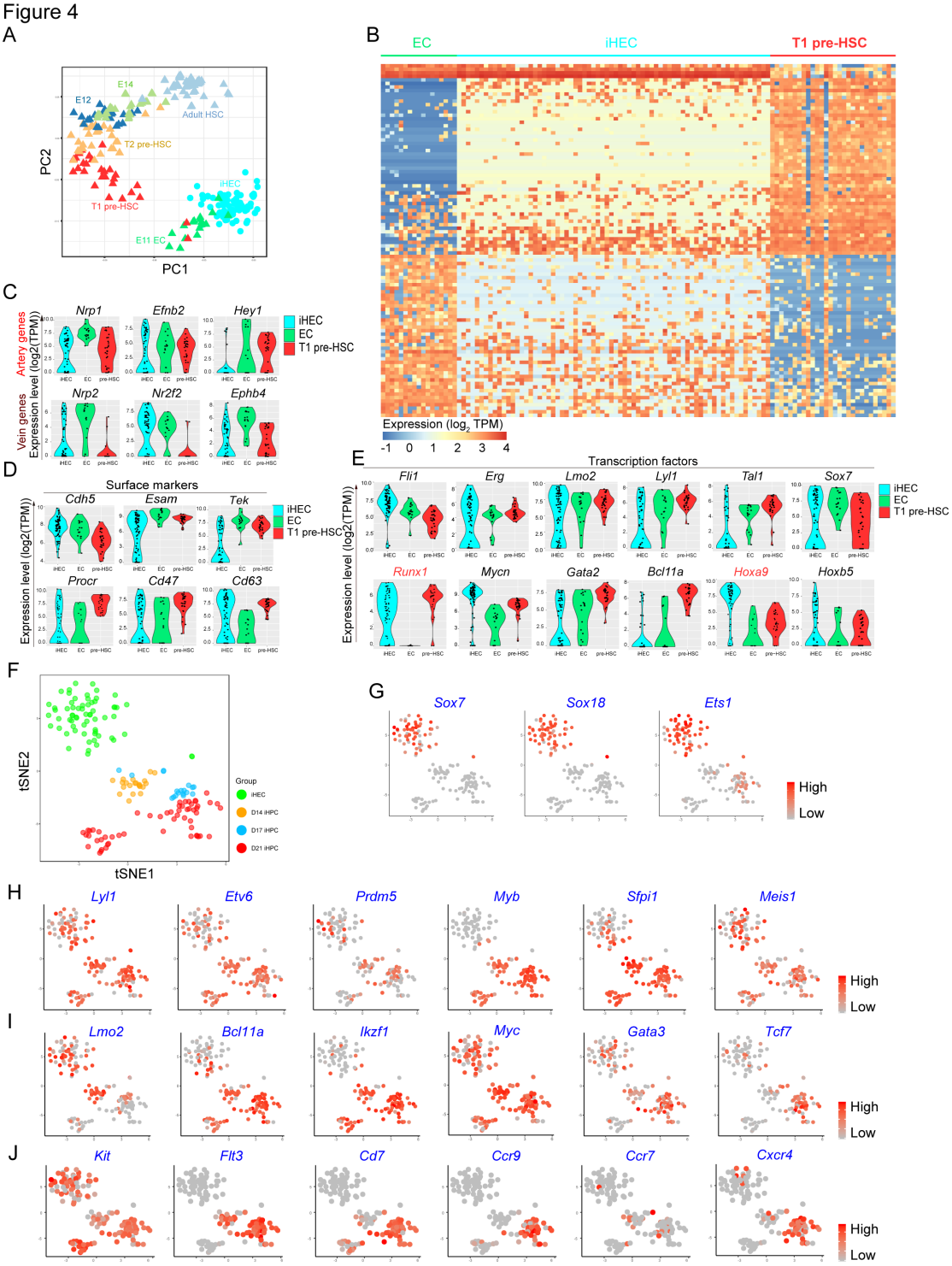

Figure 4. Single-cell Transcriptomic Characterization of iHEC and iHPC

(A) Principal component analysis (PCA) of iHEC and developmental E11 AGM-derived EC, T1 pre-HSC, T2 pre-HSC, E12 HSC, E14 HSC, and adult HSC. The single-cell RNAseq data were aligned to the mouse genome mm10 with Hisat2. The output

sam files were sorted with samtools. The TPM values of iHEC (n = 70), natural E11 AGM-derived EC (n = 17), T1 pre-HSC (n = 28), T2 pre-HSC (n = 32), E12 HSC (n = 21), E14 HSC (n = 32) and adult HSC (n = 47) single-cell RNA-Seq data were calculated with Stringtie package. ComBat from sva package was applied to remove the batch effect. Genes with TPM value > 1 in at least 3 samples were kept. Top 1000 genes ranked by standard deviation were used for PCA (stats, R package) and graphed (ggplot2, R package). Cell types were defined as: embryonic EC ($CD31^{+}$VE-$cadherin^{+}CD41^{-}CD43^{-}CD45^{-}Ter119^{-}$), T1 pre-HSC ($CD31^{+}CD45^{-}CD41^{low}$c-$kit^{+}CD201^{high}$), T2 pre-HSC ($CD31^{+}CD45^{+}$c-$Kit^{+}CD201^{+}$), E12 HSC ($Lin^{-}$Sca-$1^{+}CD11b^{low}CD201^{+}$), E14 HSC ($CD45^{+}CD150^{+}CD48^{-}CD201^{+}$), and adult HSC ($CD45^{+}CD150^{+}CD48^{-}CD201^{+}$).

(B) The expression of the top 100 genes contributing most to PC2 (50 genes for each direction). The expression value (TPM) of each gene was converted by log2 and illustrated by pheatmap (R package). One column represents one cell repeat.

(C) Violin plots show the expression profile of selected artery (A) and vein (V) related genes in single iHEC. The expression value (TPM) of each gene was converted by log2 and illustrated by ggplot2 (R package). One point represents one cell.

(D) Violin plots show the expression profile of selected surface markers in single iHEC. The expression value (TPM) of each gene was converted by log2 and illustrated by ggplot2 (R package). One point represents one cell.

(E) Violin plots show the expression profile of selected transcription factors related to hematopoietic development in single iHEC. The expression value (TPM) of each gene

was converted by log2 and illustrated by ggplot2 (R package). One point represents one cell.

(F) Two-dimensional tSNE analysis of iHEC and iHPC single-cell RNA-Seq. For single-cell RNA-Seq, the iHEC were collected on day 11, and the iHPC were collected at Day14, 17 and 21. The tSNE was performed by Rtsne (R package) and illustrated by ggplot2 (R package). The expression value (TPM) of each gene was converted by log2 and illustrated by ggplot2 (R package). Each dot represents one cell. The TPM values of iHEC (n = 65), iHPC at Day14 (n = 21), Day17 (n = 18) and Day21 (n = 56) from single-cell RNA-Seq data were calculated with Stringtie package. Cell types were defined as: iHEC $CD31^{+}CD41^{low}CD45^{-}$c-$kit^{+}CD201^{high}$; Day14 and Day17 iHPC, $CD45^{+}$Lin(Ter119/Gr1/F4-80/CD2/CD3/CD4/CD8/CD19/FcεRIα)$^{-}$; Day21 iHPC $Ter119^{-}CD45^{+}$c-kit^{+} $CD127^{+}$.

(G) tSNE analysis of the expression pattern of selected endothelia-related transcription factors in iHEC and iHPC.

(H) tSNE analysis of the expression pattern of selected hematopoietic-related transcription factors in iHEC and iHPC.

(I) tSNE analysis of the expression pattern of selected T cell development-related transcription factors in iHEC and iHPC at Day14, Day17, and Day21.

(J) tSNE analysis of the expression pattern of selected lymphopoiesis-related surface protein-coding genes in iHEC and iHPC at Day14, Day17, and Day21.

Figure 5

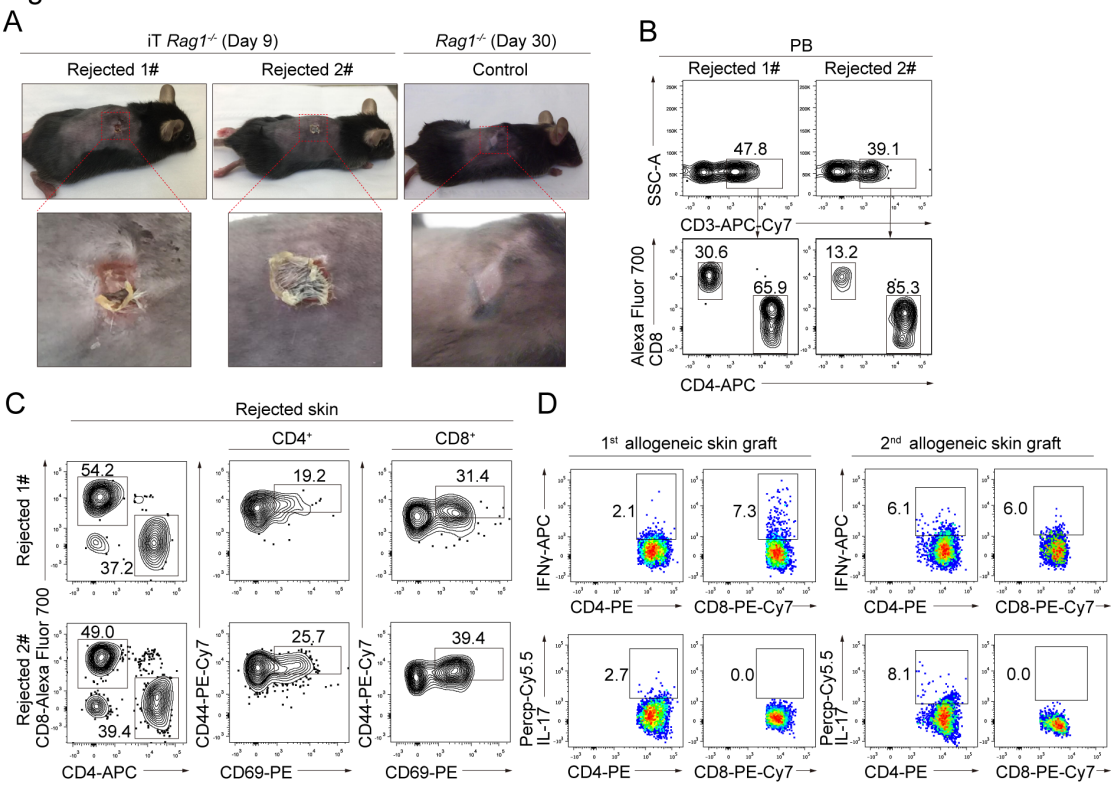

Figure 5. iT Cells Reject Allogeneic Skin in Adoptively Transferred *Rag1*$^{-/-}$ Mice

(A) The images of allogeneic skin grafts. Representative images of rejected allogeneic skin tissues on ESC-iT-*Rag1*$^{-/-}$ (day 9) mice (n = 2) and grafted skin tissue on control *Rag1*$^{-/-}$ mice (day 30) were shown. Eight-week-old *Rag1*$^{-/-}$ mice (C57BL/6 background) were transplanted with 5 million CD4^{+} and CD8^{+} ESC-iT cells by retro-orbital vein injection. The allogeneic skin sections from the bottom of BALB/c mouse tail were grafted into the back of the *Rag1*$^{-/-}$ recipient mice at day 4 after the ESC-iT cell transfer.

(B) Flow cytometry analysis of the ESC-iT cells in peripheral blood (PB) of adoptively ESC-iT transferred *Rag1*$^{-/-}$ recipients nine days after the allogeneic skin grafted. Plots of two representative mice are shown.

(C) Flow cytometry analysis of the activation status of the ESC-iT cells in the rejected allogeneic skin tissues. The rejected allogeneic skin tissues were from the adoptively

877 ESC-iT transferred *Rag1*$^{-/-}$ recipients nine days after the allogeneic skin grafted. The
878 single cells were isolated from the rejected skin tissues after digestion by collagenase I.
879 The activated ESC-iT cells were defined as CD4^{+}/CD8^{+} CD44^{high} CD69^{+}. Rejected skin
880 tissues from two representative ESC-iT transferred *Rag1*$^{-/-}$ mice were analyzed.
881 (D) Flow cytometry analysis of the intracellular cytokine IFNγ and IL-17 secreted by
882 the CD4^{+} or CD8^{+} ESC-iT cells in rejected allogeneic skin tissues. 1st allogeneic skin
883 grafts were analyzed at day 9 and 2nd allogeneic skin grafts were analyzed at day 6 after
884 skin transplantation. Data from primary and secondary rejected skin tissues from one
885 representative ESC-iT cells transferred *Rag1*$^{-/-}$ mouse are shown.

Figure 6

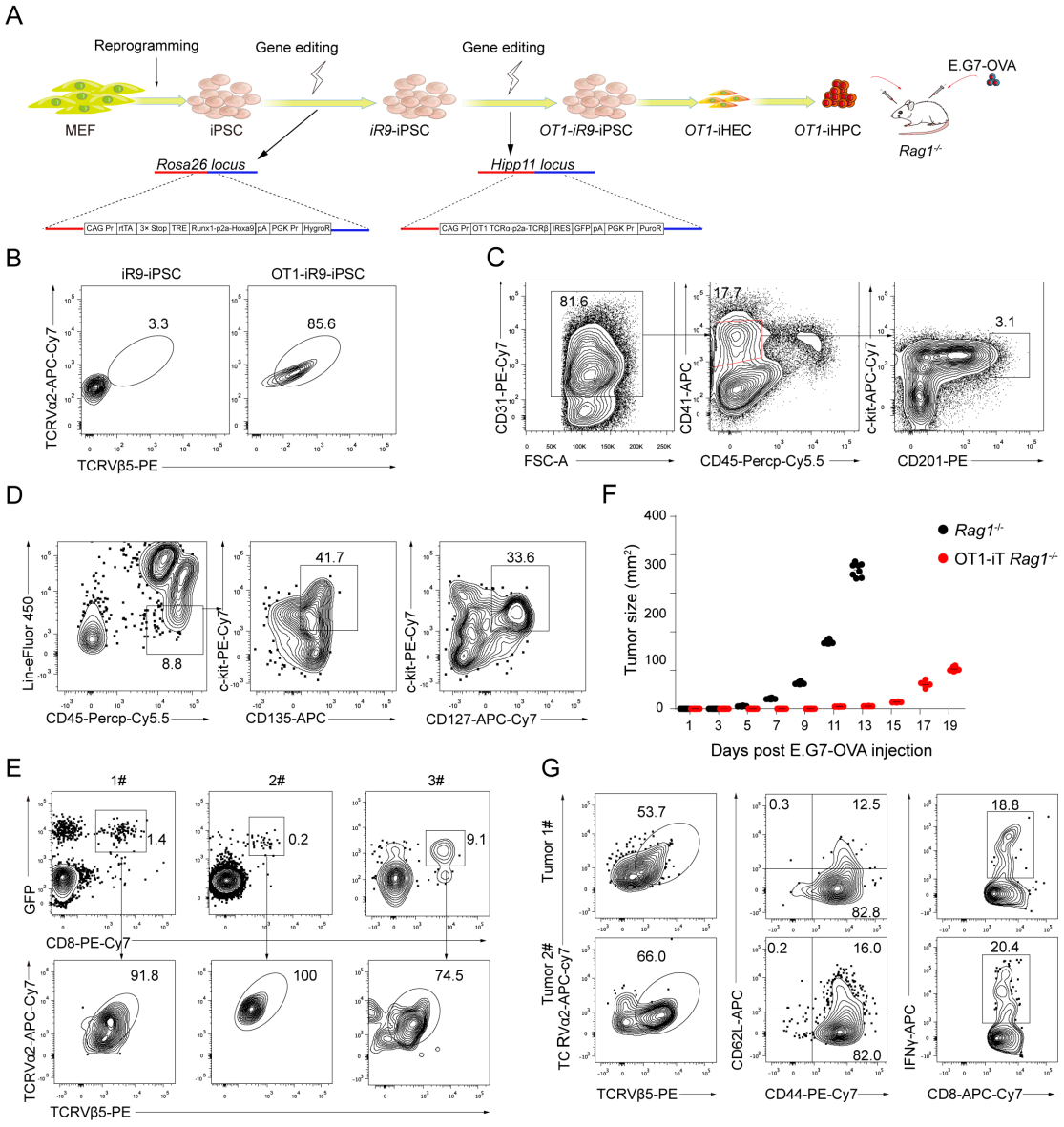

Figure 6. OT1-iT Cell Therapy Suppresses the Solid Tumor Growth in Mice Transplanted with E.G7-OVA Cells

(A) Schematic diagram of OT1 engineered iT cells for anti-tumor therapy. Mouse MEF cells were isolated from CD45.2^{+} C57BL/6 mouse and reprogrammed into iPSC with Oct4, Klf4, and Sox2 retro-viruses. Then a *rtTA-TRE-Runx1-Hoxa9-HygroR* DNA cassette was inserted into the *Rosa26 locus*. The *iR9*-iPSC clones were selected by hygromycin B (150 μg/ml). Next, a *CAG-OT1-IRES-GFP-PuroR* expression element

was inserted into the *Hipp11 locus* of *iR9*-iPSC. The OT1-*iR9*-iPSC clones were further selected by puromycin (1 µg/ml). OT1-*iR9*-iPSC results in the production of $CD8^+$ T cells carrying TCRVα2 and TCRVβ5 (MHC class I-restricted, ovalbumin-specific TCR). OT1-*iR9*-iPSC-derived iHEC were induced into iHPC (OT1-iHPC) as described in material and method sections. The iHPC were injected into irradiated (4.5 Gy) *Rag1*$^{-/-}$ recipient mice (3 million/mouse, 8-10-week-old C57BL/6 background). E.G7-OVA tumor cell line (C57BL/6 background) were transplanted into the groin of the *Rag1*$^{-/-}$ (n = 8) or OT1-iT-*Rag1*$^{-/-}$ (n = 8) by subcutaneous injection (0.2 million/mouse) six weeks after OT1-iHPC transplantation.

(B) TCRVα2 and TCRVβ5 expression in OT1-*iR9*-iPSC measured by intracellular staining. The *iR9*-iPSC was used as negative control.

(C) Sorting gates of the *OT1-iR9*-iPSC-derived iHEC population at day 11. The cells were enriched by streptavidin-beads recognizing biotin-CD31 before sorting. Representative plots from three independent experiments are shown.

(D) Immuno-phenotypes of pre-thymic progenitors in induced hematopoietic progenitor cells from *OT1-iR9*-iPSC-derived iHEC after ten-day maturation. Representative plots from three independent experiments are shown. Lin was defined as $CD2^-CD3^-CD4^-CD8^-CD11b^-Gr1^-Ter119^-CD19^-NK1.1^-TCR\gamma\delta^-$. pre-thymic progenitors were defined as $Lin^-c\text{-}kit^+CD127^+/CD135^+$.

(E) TCRVα2 and TCRVβ5 expression of iT cells in PB of *Rag1*$^{-/-}$ mice 4 weeks after transplantation of *OT1-iR9*-iPSC-derived iHPC. Three representative mice from three independent experiments were analyzed.

(F) Tumor growth in *Rag1*$^{-/-}$ and OT1-iT-*Rag1*$^{-/-}$ mice. E.G7-OVA cells were transplanted into the groin of the *Rag1*$^{-/-}$ (n = 8) or OT1-iT-*Rag1*$^{-/-}$ mice (n = 8) by subcutaneous injection (0.2 million/mouse). The length and width of the tumors were measured every other day by a caliper, and each tumor size was calculated as length × width (mm^2). Mice with tumor size larger than 20 mm at the longest axis were euthanized for ethical consideration. *** $P < 0.001$ (independent t-test, two-tailed).

(G) Characterization of the OT1-iT cells in the tumors. The tumors were isolated at day 19 after injection and disaggregated by collagenase IV to single cell suspensions. The effector iT cells were defined as CD44+CD62L-. The memory iT cells were defined as CD44+CD62L+. IFNγ secreted by CD8+ OT1-iT cells in the tumors were intra-cellular stained. Representative plots from two tumors are shown.

SUPPLEMENTARY FIGURES AND LEGENDS

Supplementary Figure 1

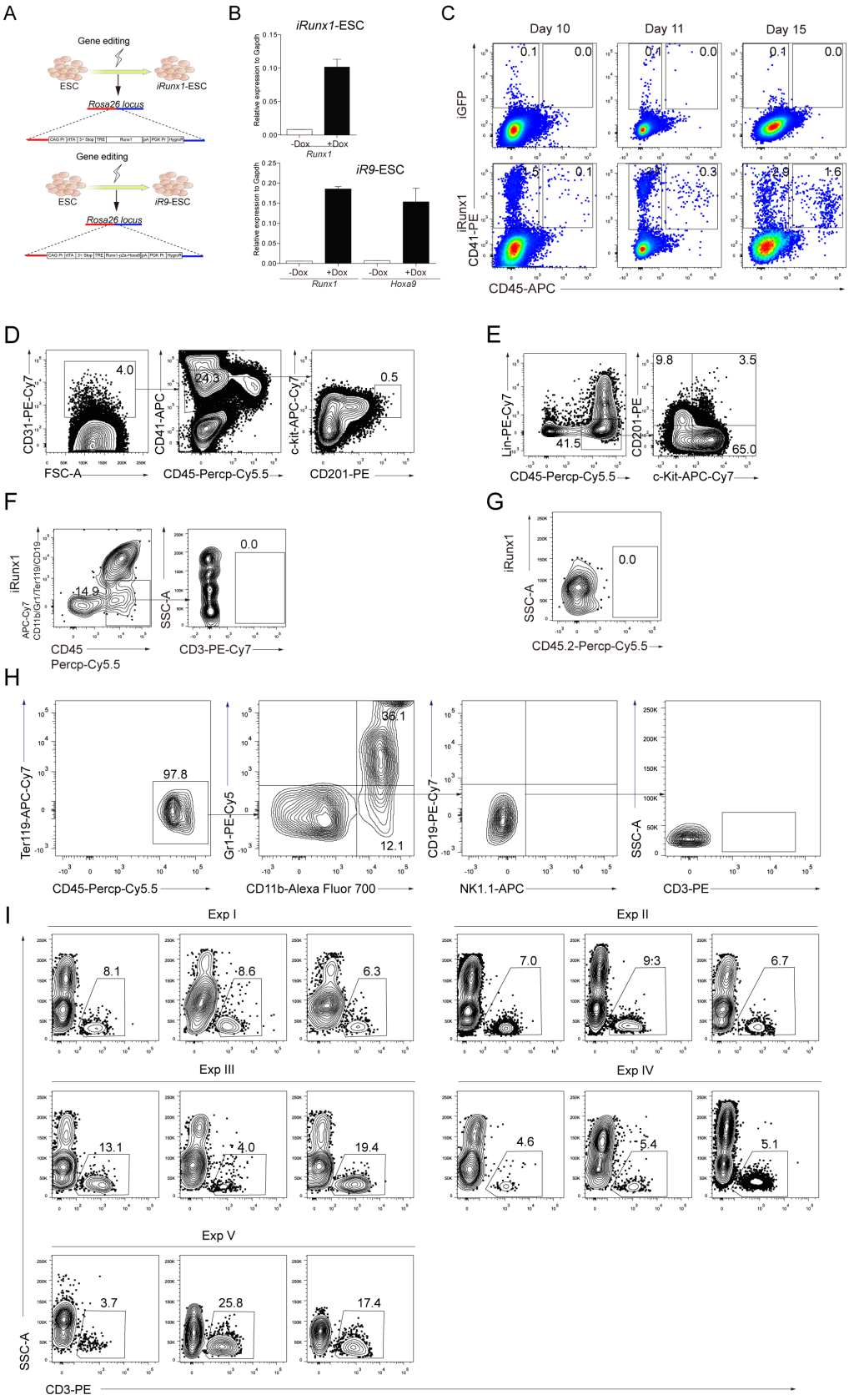

Figure S1. Transcription Factor Runx1 as the Starting Candidate for iT Cell Regeneration

(A) Schematic diagram of iRunx1-ESC and iRunx1-p2a-Hoxa9 (*iR9*)-ESC construction. A rtTA-TRE-Runx1-HygroR DNA cassette or rtTA-TRE-Runx1-Hoxa9-HygroR DNA cassette was inserted into the *Rosa26 locus* of CD45.2$^+$ C57BL/6 mouse ESC by homologous recombination. The *iRunx1*- or *iR9*-ESC clones were selected by hygromycin B (150 μg/ml).

(B) Q-PCR analysis of the expression of Runx1 in iRunx1-ESC, and the expression of Runx1 and Hoxa9 in *iR9*-ESC after doxycycline induction.

(C) Runx1 expression promotes endothelial to hematopoietic transition. CD41$^+$CD45$^-$ and CD41$^+$CD45$^+$ populations of iGFP-ESC-derived and iRunx1-ESC-derived cells were analyzed at day 10, day 11 and day 15 by flow cytometry.

(D) Sorting gates of iRunx1 ESC-derived iHEC population at day 11. Representative plots from three independent experiments are shown.

(E) Immuno-phenotypes of hematopoietic progenitors from iRunx-ESC-derived iHEC after ten-day maturation. Representative plots from four independent experiments are shown. Lin was defined as CD2$^-$CD3$^-$CD4$^-$CD8$^-$Gr1$^-$Ter119$^-$CD19$^-$NK1.1$^-$TCRγδ$^-$. Hematopoietic progenitors were defined as CD45$^+$Lin$^-$c-kit$^+$CD201$^+$.

(F) The failure of iT cell induction from iRunx1-ESC-derived iHEC.

(G) iRunx1-ESC-derived iHEC failed to contribute any hematopoietic in B-NDG mice four weeks after transplantation. One million iHEC-derived hematopoietic cells were transplanted into individual B-NDG mice (CD45.1$^+$) irradiated by X-ray (2.25 Gy). One

representative mouse was analyzed.

(H) Lineage characterization of bulk cells collected at day 10 after coculture of *iR9*-ESC-derived iHEC and OP9-DL1. One representative plot from three independent experiments are shown. Myeloid cells were defined as $CD45^{+}CD11b^{+}$.

(I) Flow cytometry analysis of pluripotent stem cell-derived T cells in PB of iHPC recipients. Plots from three mice of each independent experiment (Exp I, II, III, IV, V) are shown.

Supplementary Figure 2

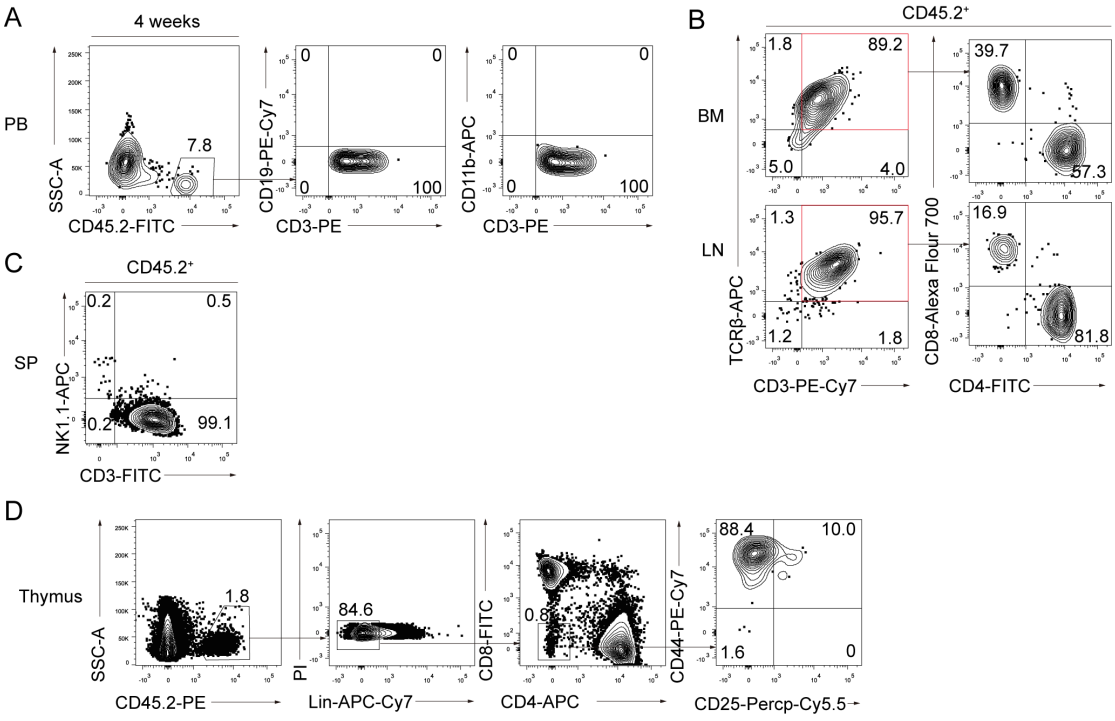

Figure S2. Day-17 iHPC Reconstitutes T Lymphopoiesis *in vivo*

(A) Induced T cells (iT) in PB of B-NDG mice were analyzed by flow cytometry 4 weeks after transplantation. One million iHPC from Day 17 in the presence of OP9-DL1 feeder cells were transplanted into individual B-NDG mice ($CD45.1^{+}$) irradiated by X-ray (2.25 Gy). One representative mouse from three independent experiments were analyzed.

(B) Flow cytometry analysis of the mature iT cells in bone marrow (BM) and lymph node (LN) of B-NDG mice transplanted with iHPC. Each B-NDG mouse was transplanted with one million iHPC collected at day 6 in the presence of OP9-DL1 feeder cells. Representative mouse was sacrificed and analyzed 5 weeks after transplantation. Data from one mouse are shown.

(C) Flow cytometry analysis of induced NK (iNK) cells and induced T cells (iT) in spleen (SP) of B-NDG mice transplanted with iHPC. Each B-NDG mouse was transplanted with one million iHPC collected from day-6 co-culture with OP9-DL1. Representative mouse was sacrificed and analyzed 5 weeks after transplantation. iNK cells were defined as $CD45.2^{+}NK1.1^{+}CD3^{-}$. Data from one representative mouse were shown.

(D) Flow cytometry analysis of induced double-negative T lymphocytes (iDN) cells in the thymus of B-NDG mice transplanted with iHPC. Each B-NDG mouse was transplanted with one million iHPC after six-day co-culture with OP9-DL1. Representative mouse was sacrificed and analyzed 5 weeks after transplantation. Data from one representative mouse from three independent experiments are shown. Lin was defined as $Ter119^{-}CD11b^{-}Gr1^{-}CD19^{-}B220^{-}NK1.1^{-}TCR\gamma\delta^{-}$.

Supplementary Figure 3

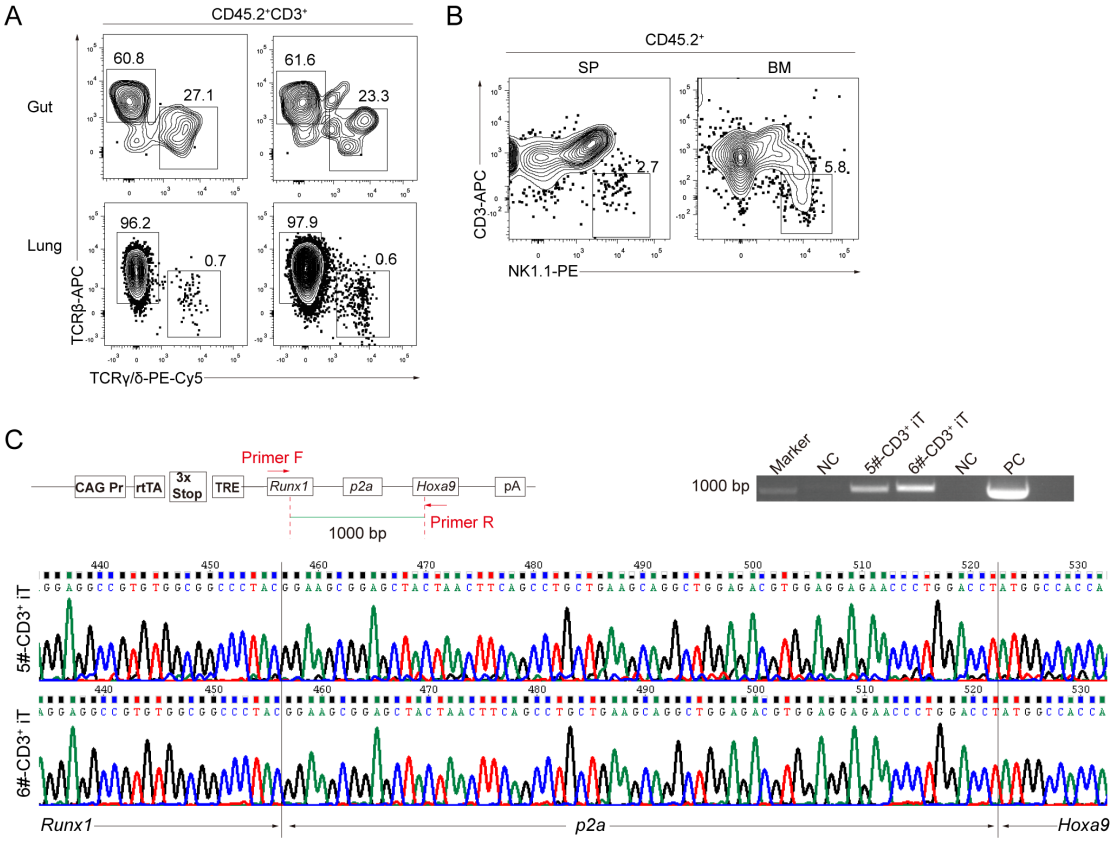

983

984 **Figure S3. Characterization of iHEC-derived iT and iNK Cells in B-NDG**

985 **Recipients**

986 (A) Flow cytometry analysis of γδ-iT and β-iT cells in the gut and lung tissues of B-

987 NDG mice transplanted with ESC-derived hematopoietic cells. Each B-NDG mouse

988 was transplanted with one million iHEC-derived hematopoietic cells and fed with

989 Doxycycline (1 mg/ml) for sustaining 6 weeks. Representative mouse was sacrificed

990 and analyzed at 6 weeks after transplantation. Data from two representative mice are

991 shown.

992 (B) Measurement of induced NK cells in spleen (SP) and bone marrow (BM) of B-

993 NDG mice transplanted with iHPC. Pluripotent stem cell-derived NK cells were

994 defined as $CD45.2^{+}NK1.1^{+}CD3^{-}$. Plots from one representative B-NDG mouse six

995 weeks after transplantation of iHPC are shown.

996 (C) Genotype sequencing of the Runx1-p2a-Hoxa9 element of the sorted iT cells.
997 Genomic PCR were performed using primer pairs flanking the inserted Runx1-p2a-
998 Hoxa9 sequence element, and genome template (200 ng) of 20,000 sorted iT cells from
999 the spleen of iT-B-NDG mice. The sequencing results were visualized by chromas
1000 software. PCR products of iT cells from two iT-B-NDG mice were sequenced and
1001 shown.

Supplementary Figure 4

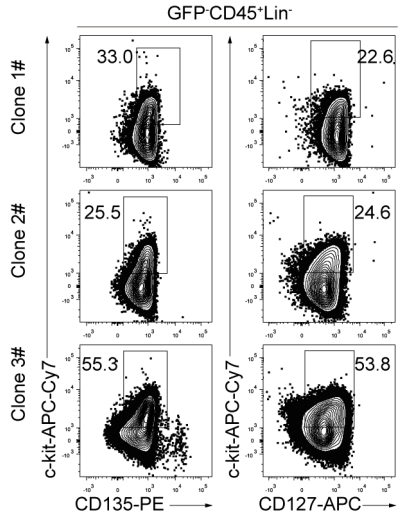

1002

1003 **Figure S4. Single iHEC from *iR9*-ESC Gives Rise to iHPC *in vitro***

1004 Immuno-phenotypes of pre-thymic progenitors in induced hematopoietic progenitor
1005 cells from *iR9*-PSC-derived iHEC after ten-day maturation. Three representative clones
1006 from two independent experiments were analyzed. Lin was defined as $CD2^-CD3^-CD4^-$
1007 $CD8^-CD11b^-Gr1^-Ter119^-CD19^-NK1.1^-TCR\gamma\delta^-$. pre-thymic progenitors were defined
1008 as $Lin^-c\text{-}kit^+CD127^+/CD135^+$.

Supplementary Figure 5

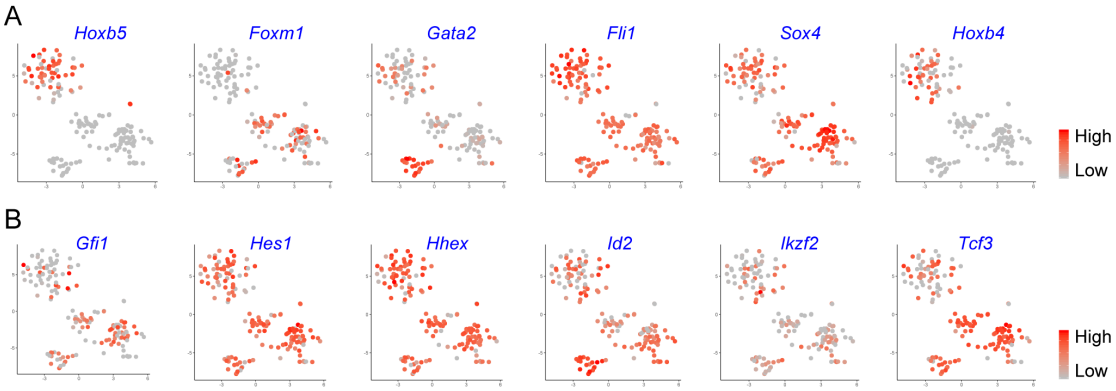

Figure S5. Time-course Expression Patterns of Hematopoietic and Lymphopoietic Development-related Transcription Factors in Single iHEC and iHPC Derived from *iR9*-ESC

(A) tSNE analysis of the expression pattern of selected hematopoietic-related transcription factors in iHEC and iHPC.

(B) tSNE analysis of the expression pattern of selected T cell development-related transcription factors in iHEC and iHPC at Day14, Day17, and Day21.

Supplementary Figure 6

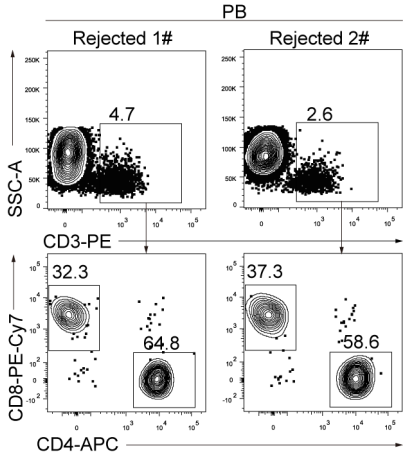

Figure S6. iT Cells in PB of iT-*Rag1*$^{-/-}$ Mice 30 Days after 1st Allogeneic Rejection

Flow cytometry analysis of the iT cells in peripheral blood (PB) of iT transferred *Rag1*$^{-/-}$ recipients 30 days after 1st grafted allogeneic skin rejection. Plots of two

representative mice are shown.

Supplementary Figure 7

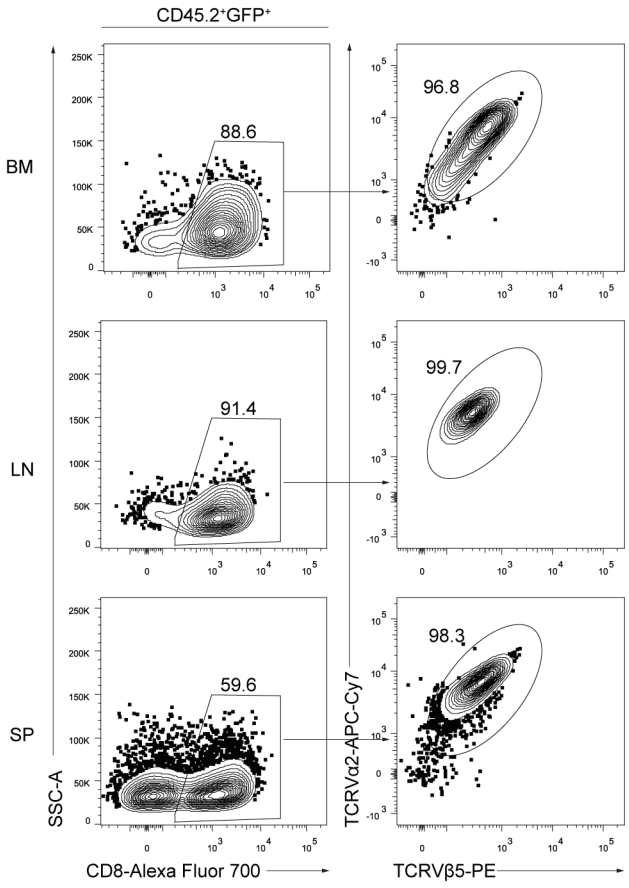

Figure S7. Distributions of OT1-iT Cells in the BM, LN and SP of OT1-iT *Rag1*$^{-/-}$ Mice 19 Days after E.G7-OVA Tumor Cell Injection

Rag1$^{-/-}$ mice were transplanted with iHPC (3 million/mouse) 4 weeks before E.G7-OVA tumor cell injection. OT1-iT *Rag1*$^{-/-}$ mice carrying tumors were sacrificed 19 days after E.G7-OVA tumor cell injection. TCRVα2 and TCRVβ5 on CD8^{+} iT cells were analyzed in the bone marrow (BM), lymph node (LN) and spleen (SP) of the OT1-iT *Rag1*$^{-/-}$ mice. Plots of one representative mouse are shown.

Supplementary Figure 8

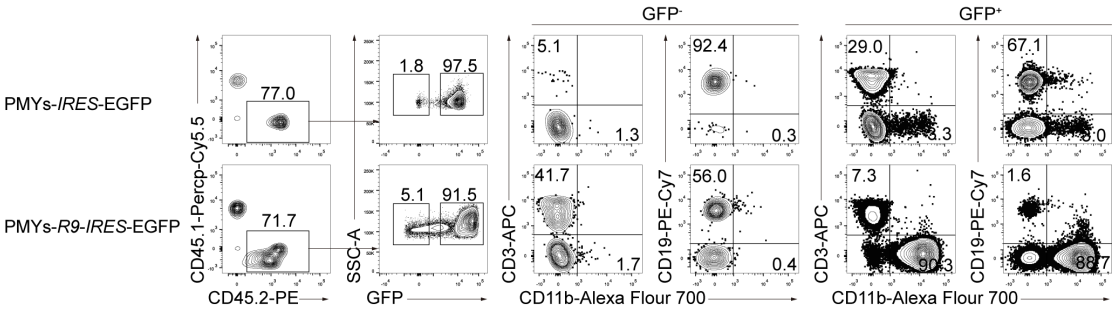

Figure S8. Overexpression of Tandem *Runx1-p2a-Hoxa9* in Natural HSC Leads to Myeloid- Instead of Lymphoid-biased Hematopoietic

Lineage contribution of HSC transduced with PMYs-IRES-EGFP or PMYs-R9-IRES-EGFP retrovirus. E14.5 fetal liver HSPCs (FL-HSPCs) were enriched by Lineage (CD2/3/4/8/B220/CD19/Ter119/Gr1) cell deletion and were infected with PMYs-IRES-EGFP or PMYs-R9-IRES-EGFP retrovirus. Half million HSPC transduced with the related viruses were transplanted into the individual CD45.1 C57BL/6 mice irradiated by X-ray (6.5 Gy). Peripheral blood cells were analyzed 16 weeks after transplantation cells.